UNIVERSITY OF OKLAHOMA

GRADUATE COLLEGE

EXPERIMENTAL STUDY OF ASPHALTENE ACCUMULATION IN A SANDSTONE

CORE PLUG.

A THESIS

SUBMITTED TO THE GRADUATE FACULTY

IN PARTIAL FULFILLMENT OF THE REQUIREMENTS FOR THE

DEGREE OF

MASTER OF SCIENCE

By

PAPA ADAMA LO
NORMAN, OKLAHOMA
2021

EXPERIMENTAL STUDY OF ASPHALTENE ACCUMULATION IN A SANDSTONE

CORE PLUG.

A THESIS APPROVED FOR THE

MEWBOURNE SCHOOL OF PETROLEUM AND GEOLOGICAL ENGINEERING

BY THE COMMITTEE CONSISTING OF

Dr. Ali O. Tinni, Chair

Dr. Rouzbeh G. Moghanloo

Dr. Deepak Devegowda

By the grace of the Almighty,

Acknowledgements

Table of Contents

List of Figures

x

Abstract

Hydrocarbon production leads to the disturbance of several thermodynamic equilibriums including the destabilization of crude oil. Asphaltenes precipitation, aggregation and deposition inside the hydrocarbon reservoirs remains challenging issue due to the multiple factors controlling these processes. Despite the fact formation damage due to asphaltenes accumulation could be highly detrimental to production and/or injection operations, there is no experimental data on asphaltene accumulation during gas and oil flow at high pressure in porous media.

To address this lack of experimental data, we have designed and assembled an experimental apparatus that can be used to study the asphaltene accumulation in porous media during oil and gas flow. We have used this apparatus to investigate the impact of pressure and flowrate on the asphaltene deposition process in a Berea sandstone core plug. Moreover, we also evaluated the efficacy of surfactant injection to prevent asphaltene accumulation within the core plug.

The impacts of pressure were evaluated by injecting simultaneously crude oil and a mixture of 72% of methane and 28% of ethane at pressures of 4,500 psi (1.07% of MMP), 3,570 psi and 3,150 psi at a constant flowrate of 0.025 ml/min and temperature of 170°F. This co-injection of crude oil and the gas mixture was also conducted at flowrate of 0.25 ml/min to evaluate the impact of flowrate. To evaluate the use of surfactant to prevent asphaltenes accumulation, the co-injection of oil and gas was conducted by saturating the core sample with brine containing surfactants (1gpt and 10 gpt) before the establishment of S_{wir}. After core flooding to establish S_{wir}, co-injections of oil and the gas mixture were conducted 300 psi above the MMP at precisely 4,500 psi.

Our experiments show that the permeability loss due to asphaltenes accumulation is more severe as the injection pressure approaches the MMP value. At pressures lower than the MMP, a process of accumulation and re-solubilization is observed. We also observed that an increase of flowrate

from 0.025 ml/min to 0.25 ml/min prevents the deposition of asphaltenes, indicating that formation damage by asphaltenes is a slow process that can be prevented by increasing injection or production rates. The injection of surfactants did not prevent asphaltenes accumulation. With the 10 gpt surfactant solution, we observed an occurrence of formation damage earlier than in the cases where the sample was initially saturated with the 1 gpt solution and with brine.

CHAPTER 1: INTRODUCTION

1.1. Motivation and Problematic statement:

Hydrocarbon production and gas injection often affect the equilibrium between the different crude oil components. Crude oil is essentially constituted by saturate, aromatic, resin and asphaltene (SARA). Asphaltenes are the heaviest and most polar compounds of crude oil (Mirzayi et al., 2008; Akbarzadeh et al., 2007; Mullins, 2011). They share a special relationship with another polar aromatic component which is the resins. In fact, the asphaltenes and resins fractions are chemically bonded. This bond promotes the stability of the asphaltene molecules in crude oil. However, the asphaltene-resin bonds do not resist the pressure reduction during reservoir depletion or temperature changes in the production tubing, thus leading to asphaltenes precipitation and deposition in hydrocarbon reservoirs as well as production tubing and pipelines. Asphaltenes are insoluble in light n-alkanes such as n-pentane and n-heptane, but they are soluble in aromatic solvents such as toluene, benzene, and xylenes (Fakher et al., 2019; Goual, 2012).

In the near wellbore region, asphaltene molecules can be deposited in quantities large enough to reduce the hydraulic radius of the pores and/or plug the pore throats, hence reducing the effective permeability of the formation (Figure 1.1).

Asphaltene precipitation and deposition in petroleum reservoirs, production tubing and transportation pipelines lead to significant production losses (Riazi and Zare, 2018; Ali and Ghannam, 1981; Angle and Long, 2006; Hirschberg et al., 1984). This added to the workover required to resume production cause enormous financial losses to the oil and gas industry.
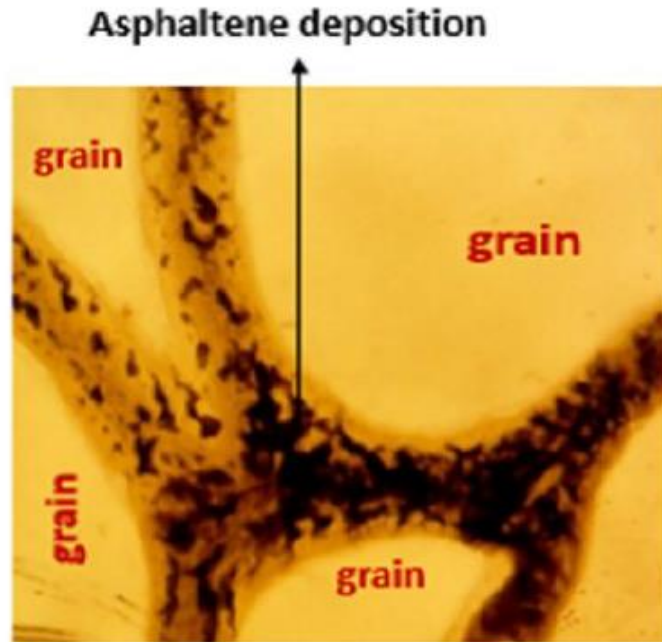
Figure 1.1. Asphaltenes aggregation plugging reservoir pores throat in a micromodel (Shahsavar et al., 2020).

1.2. Research objectives:

Previous studies on asphaltenes behavior in crude oil have focused on:

- The determination of asphaltenes precipitation onset (Hirschberg et al., 1984; Buckley, 1996; Maqbool et al., 2011; Wang and Civan, 2001)

- Improving the understanding of asphaltene deposition on pipe surfaces (Ashoori et al., 2016; Hashmi et al., 2015)

- Evaluating asphaltenes accumulation in porous media (Ali and Islam, 1997; Kord et al., 2012; 2013)

- The development of simulation methods for asphaltenes deposition in pipes and porous media (Leontaritis and Mansoori, 1987; Burke et al., 1988; Leontaritis et al., 1994).

Among the topics addressed by the previous studies, asphaltenes precipitation and accumulation in porous media is the subject with the largest knowledge gap. This lack of knowledge is essentially due to the lack of experimental data on asphaltene accumulation during oil and gas flow at high pressures in porous media.

To improve the understanding of asphaltene precipitation and deposition in porous media, we have conducted a study that can be divided into 3 main parts:

- ✓ Investigation of the role of pressure on the asphaltenes accumulation in porous media.
- ✓ Study of the impact of flow rate on the asphaltenes accumulation in porous media.
- ✓ Evaluation of the efficacy of surfactant injection to prevent asphaltenes accumulation in porous media.

1.3. Organization of the thesis

Chapter 2 of this thesis presents a literature review of the relevant previous studies on asphaltene precipitation and accumulation. It will include a description of the molecular structure of asphaltenes and the factors leading to their precipitation. We will review the investigations conducted in order to understand asphaltenes accumulation in general, and in porous media particularly. General strategies used to mitigate the accumulation of asphaltenes will be introduced. We will also present an overview of the modeling methods that can be used to model asphaltenes deposition in porous media.

Chapter 3 will present the experimental methods and procedures used in this thesis.

Chapter 4 will summarize the results of the experimental investigations on the role of pressure and flowrate on asphaltene accumulation in porous media. Moreover, it will also present the results of surfactant treatment to prevent asphaltenes accumulation.

Chapter 5 includes the summary and conclusions of the work performed during this thesis project as well as the recommendations for future studies about the asphaltenes accumulation in porous media.

CHAPTER 2: LITERATURE REVIEW

2.1. Presentation of asphaltenes

2.1.1. Introduction

Referred as "cholesterol of petroleum" by Boek et al. (2010), the term asphaltenes was originally introduced by Boussingault (1937). He described asphaltenes as the residues remaining after the distillation of bitumen. This definition implied that asphaltenes are insoluble in alcohol but soluble within a resinous oil from pine trees called turpentine. Asphaltenes have also been characterized as molecules with no boiling point (infusible), which tend to decompose when heated (Akbarzadeh et al., 2007).

Crude oil can be separated into asphaltenes and maltenes by introducing n-alkanes such as n-pentane or n-heptane. Maltenes are soluble in n-alkanes and can be subdivided in different fractions including saturates, aromatic, resins (Bearsley et al., 2004). SARA analysis is the laboratory protocol used to separate the different components of a dead crude oil into saturates, aromatics, resins and asphaltenes. During SARA analysis, asphaltenes are described as the fraction of crude oil that is soluble in aromatic solvents such as toluene but insoluble in lightweight n-alkanes such as n-pentane and n-heptane (Mirzayi et al., 2008; Akbarzadeh et al., 2007). However, asphaltenes do not have the same solubility in all n-alkanes. Asphaltenes solubility increases as the molecular weight of the n-alkane increases. Figure 2.1 shows that the lower the molecular weight of the n-alkane precipitant, the higher the amount of asphaltenes precipitated. Therefore, formation damage due to asphaltenes accumulation could be more important during gas injection for EOR purposes than during reservoir depletion.
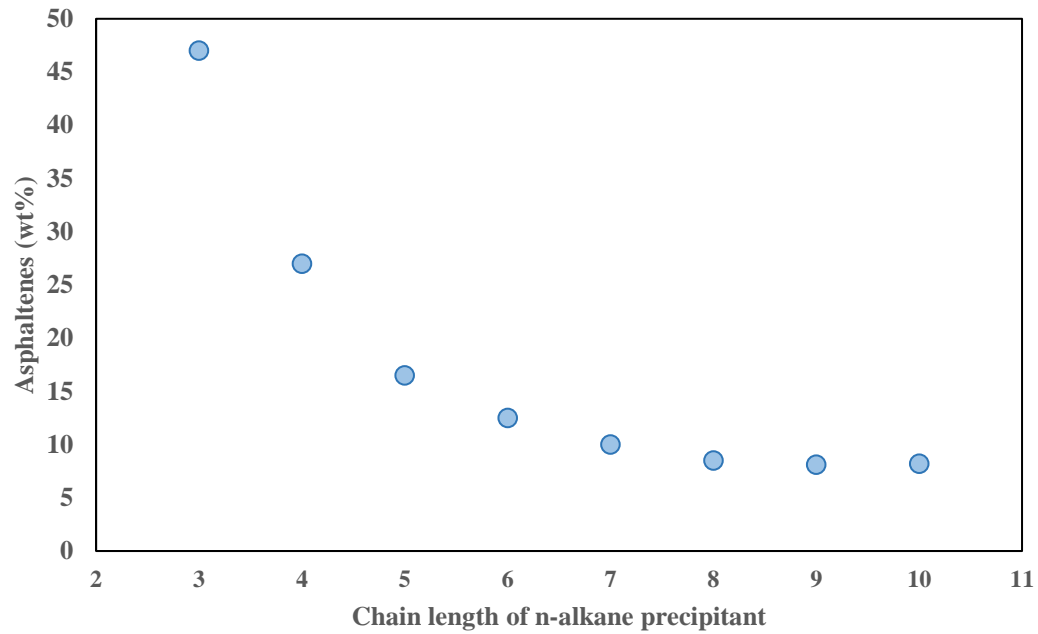
Figure 2.1. Amount of asphaltenes precipitated as function of the precipitant molecular weight. (Wang, 2000).

It is important to note that asphaltenes are the heaviest and the most polar fractions of crude oil (Mullins, 2011; Hashmi et al., 2013). In crude oil, asphaltene molecules are stabilized by the resins which are adsorbed onto the asphaltenes micelles, thus dispersing them in the fluid (Figure 2.2).
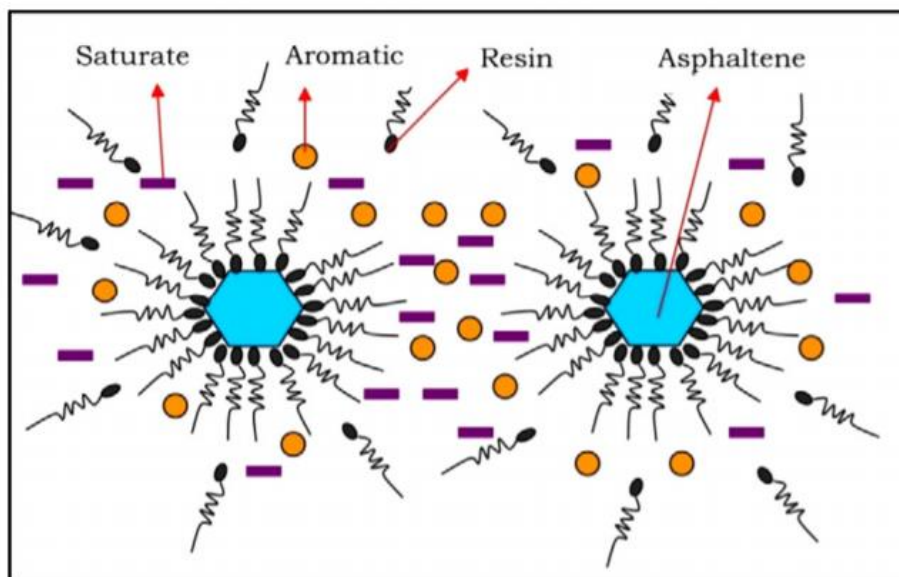
Figure 2.2. Configuration of the different fraction of crude oil. The adsorption of resins on asphaltenes (Ashoori et al., 2016).

2.1.2. Chemistry of asphaltenes

The structure of asphaltenes molecules has been a subject of controversy in the scientific community for the past decades (Fakher, 2019; Yarranton, 2005). As of now a unanimous description of its structure is still not available. Techniques such as mass spectrometry, electron microscopy, nuclear magnetic resonance, small-angle neutron and X-ray scattering, ultrasonic spectroscopy, dynamic light scattering, and gel permeation chromatography have been employed to characterize asphaltenes molecules (Akbarzadeh et al., 2007; Andrews et al., 2006).

It is generally accepted that asphaltenes have an elemental composition of carbons and hydrogens with a specific ratio of 1 to 1.2. They also contain in their structure a non-negligible percentage of heteroatoms groups and organometallic compounds (Speight, 1996; Akbarzadeh et al., 2007). The

main heteroatoms which act as polar functional groups of asphaltenes are Sulfur (S), Nitrogen (N) and Oxygen (O). While the metallic compounds may be Nickel (Ni), Vanadium (V) or Fer (Fe).

Speight and Plancher (1991) indicated that in their structure, the Oxygen heteroatom existed in acidic (carboxylic, phenolic) and in ketonic locations, and the Nitrogen heteroatom existed for most as pyrrolic and pyridinic. While the main heteroatom element which is Sulphur occurred in either aliphatic structures (sulfides and disulfides) or oxidized forms (Cimino et al.,1995). They also stated that most metals are in porphyrin structures. Asphaltenes molecules also contain one or more polyaromatic units linked by alkyl and alicyclic chains (Speight, 1996; Gray et al., 2011). These polyaromatic rings are also found in aromatic solvents unlike in the n-alkanes. This allows the dissolution of asphaltenes by aromatic solvents due to the interactions between their rings. Their insolubility in n-alkanes is due to the lack of rings in their structure.

Two different architectures of asphaltene molecules have been proposed in the literature: the continental and the archipelago (Headen et al., 2009; Boek et al., 2010). The continental structure is known to have a large central aromatic region with small alkyl chains on the periphery (Figure 2.4). And the archipelago one is associated with smaller condensed aromatic groups that are linked by bridges of alkanes (Figure 2.3) (Yarranton, 2005; Headen et al., 2009).

The molecular weight of asphaltenes molecules has been reported to be in the range of 500 g/mol to 12,000 g/mol (Waller et al., 1989; Mullins et al., 2012; Yarranton et al., 2013).
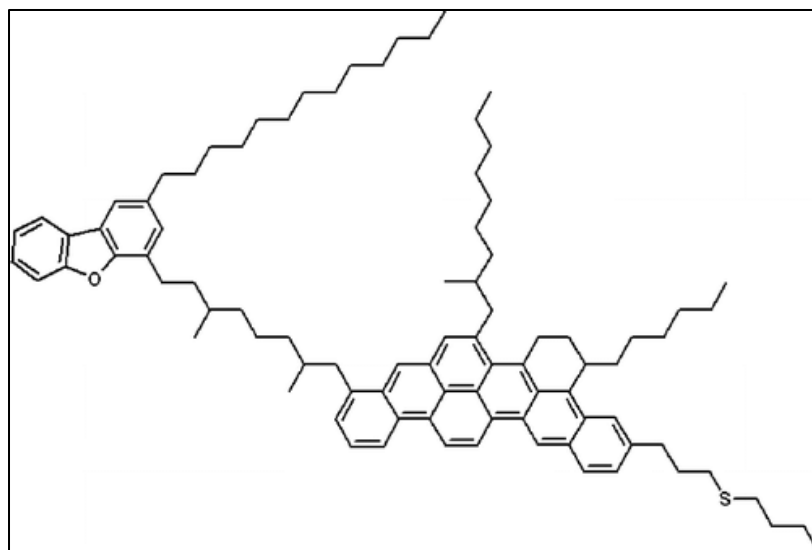
Figure 2.3. An archipelago type structure of chemical structure of asphaltene (Headen et al., 2009).
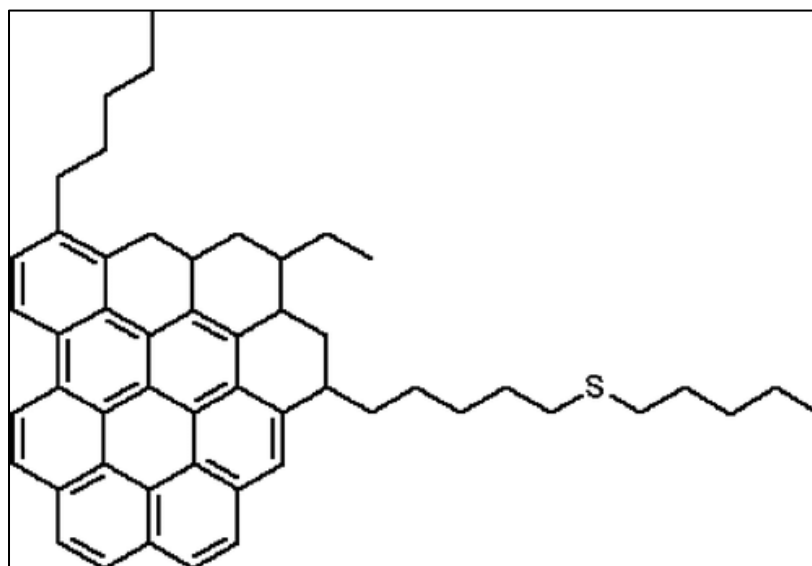
Figure 2.4. A continental type of chemical structure of asphaltene (Headen et al., 2009).

2.2. Asphaltenes precipitation and deposition

Asphaltenes can be found stable in crude oil either in a dissolved state or as colloidal dispersion. When the equilibrium between the different crude oil fractions is disturbed, the colloids start to flocculate and aggregates of asphaltenes start to form and interact with each other to generate super aggregates with larger sizes from molecular to clusters (Mullins, 2011; Fakher, 2019). When the density of the super aggregates is large enough, the aggregates will deposit. The equilibrium between the different crude oil fractions can be disturbed by factors such as pressures, temperatures, composition.

2.2.1. Impact of pressures changes on the asphaltenes precipitation

It is well known in the industry that pressure reduction during reservoir depletion is responsible for asphaltenes precipitation and deposition. Several laboratory studies have replicated the pressure depletion process to study the impact of pressure on asphaltenes precipitation (Chen et al., 2012, Burke et al. 1988, Thawer et al.,1990, Akbarzadeh et al. 2007, Ahmadi et al. 2014, Hashemi et al., 2008). Figure 2.5 shows a compilation of the data collected in some of these studies.
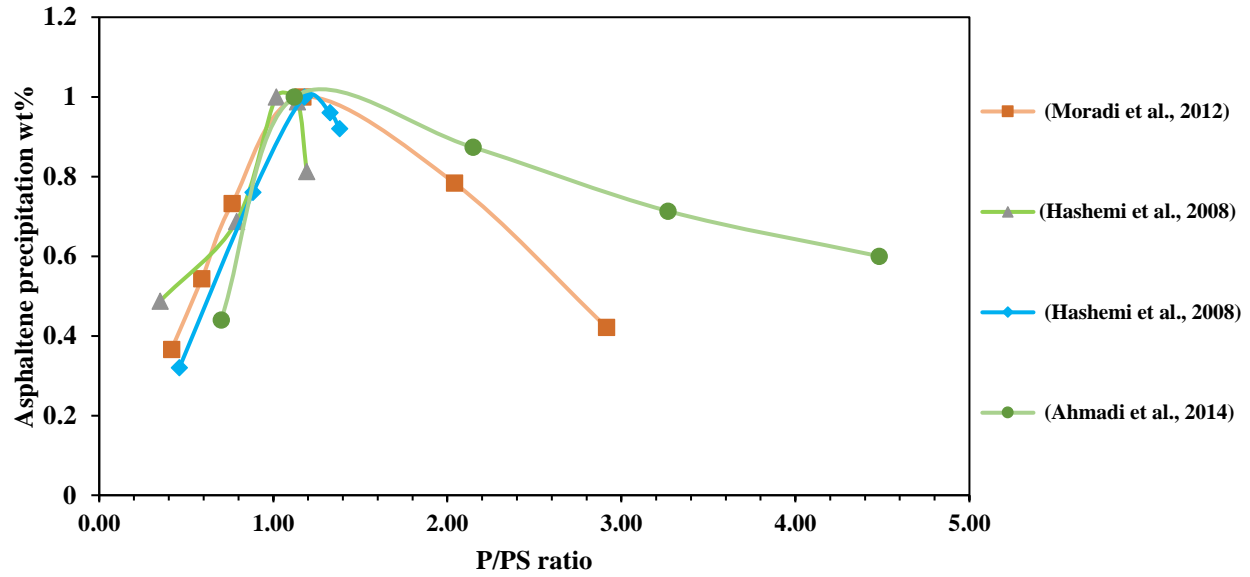
Figure 2.5. Normalized mass of asphaltenes precipitated as function of normalized pressure. The mass of asphaltenes precipitated was normalized by the maximum mass of asphaltenes precipitated during pressure depletion. The pressures were normalized by the bubble point pressure.

These studies have shown the maximum amount of asphaltenes precipitated is observed near the bubble point. Asphaltene precipitation increases as the pressure decreases toward bubble point because of the expansion of the light n-alkane fraction. Asphaltenes precipitation also reduces as the pressure decreases below the bubble point. However, in this case, the reduction in asphaltenes precipitation is due to the evaporation of the light n-alkane molecules which makes the remaining oil a better solvent for asphaltenes molecules.

2.2.2. Impact of temperature changes on the asphaltenes precipitation

Early studies on the impact of temperature changes on asphaltene precipitation seemed to be contradictory. Burke et al. (1988) found that asphaltenes solubility decreases as temperature

increases while Thomas et al. (1992) concluded that asphaltenes solubility increases as temperature increases.

To better understand the effects of temperature on the asphaltenes precipitation process Leontaritis et al. (1996) conducted a study where they considered temperature changes relative to the temperature of the reservoir from which the crude oil was extracted. At temperatures larger than the reservoir temperature, asphaltenes precipitation increases as temperature increases. However, at temperatures lower than the reservoir temperature, asphaltenes precipitation reduces as the temperature increases.

While studying the effect of temperature on the kinetics of asphaltene precipitation from crude oil, Maqbool et al. (2011) demonstrated that at higher temperatures the asphaltenes precipitation onset time is shorter.

2.3. Asphaltenes deposition

Asphaltenes may precipitate during production, enhanced oil recovery operations with gas injections, due to changes in pressure, temperatures, or crude oil composition. This precipitation often leads to flocs of aggregates which will be deposited onto pipe and pore surfaces. Figure 2.6 illustrates asphaltenes deposits on a production tubing.

Figure 2.6. Clogging of asphaltenes on a pipe (Goual, 2012).

2.3.1. Asphaltenes deposition studies using microfluidic, stainless surfaces

To study the deposition of asphaltenes, microfluidic devices and stainless surfaces are generally used to represent the porous media and pipes respectively.

Ashoori et al. (2006) used a slim stainless tube as porous medium to investigate the precipitation and reversibility of asphaltenes. They used a heavy crude oil with API of 20 with n-heptane as its precipitant. After precipitation of asphaltenes in the porous media, they flow fresh crude oil and allow the soaking for a certain time. The results they provide are, fresh oil flown back to a damaged reservoir can redissolve the precipitated asphaltenes.

Wang et al. (2004) investigated the influences of different factors of asphaltenes deposition on metallic surfaces using stainless steel capillary tubes. They found out the rate of deposition is not

affected by the length of the capillary tube used or the oil flow rate. But that higher degree of supersaturation of the mixtures, same as higher molar volume precipitants entrain a greater rate of deposition.

Hashmi et al. (2015) study the colloidal asphaltene deposition in laminar pipe flow. They did a lab-scale experiments injecting a mixture of precipitating petroleum fluid into a small metal pipe using various material and flow conditions. They assessed the deposition and clogging by measuring the pressure drop across the pipe. Their results suggest that the clogging behavior is determined by a combination of the Peclet number, volume fraction of depositing material, and the volume of the injection itself.

Using automated microfluidic devices, Chen et al. (2019) investigated the deposition of asphaltenes at different temperatures from 25 to 65 °C. They found out when the deposition temperature is increased, a decrease in the dispersity of asphaltene nanoaggregates is observed in the porous media.

2.3.2. Core flooding deposition

Formation damage due to asphaltenes deposition could have severe adverse effects on hydrocarbon production. Microfluidic devices have been used by previous authors to represent porous media in order to investigate asphaltenes accumulation in reservoir (Chen et al., 2019; Lin et al., 2017). However, these microfluidic devices do not capture the complexity of porous media. Core plugs were used by the following authors to evaluate asphaltene deposition in reservoirs rocks.

The results of these studies indicate that formation damage due to accumulation of asphaltenes can lead to 90% reduction of the initial rock permeability. Minssieux et al. (1997); Ali and Islam

(1997); Zekri and Almehaideb (2001) found that the permeability impairment was function of the rock type, original permeability, morphology of the rock sample, the fluid injection rate and asphaltenes content.

Pore plugging and adsorption are the main mechanisms leading to permeability impairment due to asphaltenes deposition. Ali and Islam, (1997), Kord et al. (2012; 2013) have shown that the surface deposition is the principal source of formation damage and that the increase in pore throat plugging reduces linearly the core sample permeability for live/dead crude oil flooding in a carbonate. However, Behbahani et al. (2013) found both mechanisms to be more important in carbonate than in sandstones reservoir. The experiments of Struchkov et al. (2018) have shown that the small size pores are more prone to plugging than the bigger pores.

Soroush et al. (2014) investigated the deposition of asphaltenes consequent to miscible and immiscible CO_2 flooding and its effect on porous media. Their results indicated at pressure above the MMP asphaltene deposition is the main factor of permeability reduction.

Using a limestone core plug, Cruz et al. (2009) reported 24% reduction of the original rock permeability when the pressure was near Bubble point.

Pak et al. (2011) studied an Iranian sandstone core under high temperature and pressure. They used three processes: recycled gas injection, CO_2 injection and natural depletion. They observed that most permeability damage is happening with the recycled gas injection while the less permeability reduction is found with the natural depletion.

Kordestany et al. (2019) investigated the formation damage in sand packs caused by solvent induced asphaltenes deposition. They saturated with crude oil the sand packs which known characteristics. N-heptane is the solvent used to flood the oil saturated sand packs and induced the

deposition. They concluded that the deposition mostly happened in areas closed to the solvent injection, so was not uniform. The deposition varied between 1 to 20 mg/1g of sand grain. And once deposited, the asphaltenes particles do not migrate through the porous media.

In many experimental studies in the literature, the flowing in the porous media was not done as identical to what we can expect from a natural hydrocarbon reservoir. This is due to numerous issues that come with the experimentations. To state just one of the main issues encountered is the deposition of asphaltenes cake in the inlet face of the core sample. This deposition mays consequently influence much of the permeability impairment results obtained through the laboratory-scale studies.

2.3.3. Computational deposition model

Some computational works associated or not with experimental procedures are done to better understand asphaltenes deposition process by simulation and modeling.

Leontaritis and Mansoori (1987) developed a thermodynamic colloidal model that allows the determination of the onset of flocculation of asphaltenes due to changes in composition or electrical phenomena. Leontaritis et al. (1994) added from their systematic approach that the asphaltene deposition envelope (ADE) concept is a useful tool in diagnosing, preventing, and mitigating asphaltene flocculation and deposition during oil recovery, processing, and transportation (Figure 2.7).
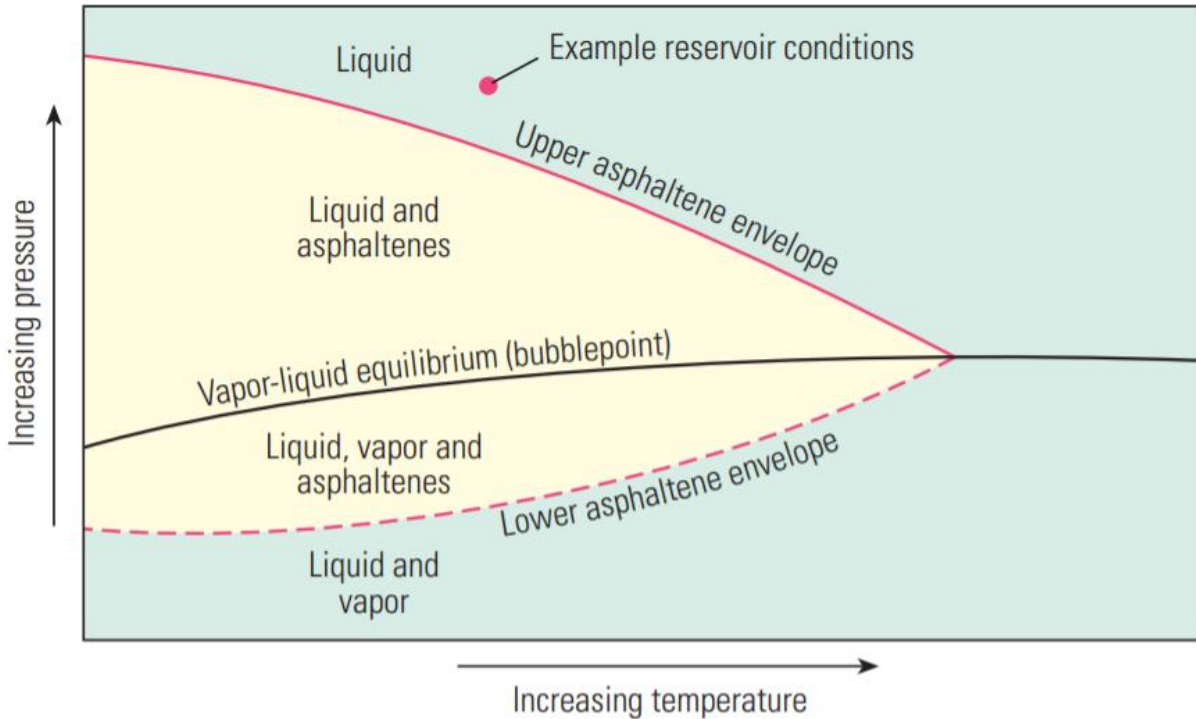
Figure 2.7. The asphaltenes deposition envelope in term of Temperature and pressure conditions.

Burke et al. (1988) proposed a model that can be used to predict the likelihood of asphaltenes precipitation forming as function of the change of composition and properties of the reservoir fluid.

Ali and Islam (1997) in their experimental study described previously, developed a mathematical model. It was based on the two main mechanisms of deposition and plugging. And The model was able to fit the experimental data.

In 1999, Wang and Civan developed a model simulating the paraffin and asphaltenes deposition in porous media. The model is validated by accurately reproducing laboratory experimental data. Following their case studies, they indicated static surface deposition mays happen even without fluid flowing. But the dynamic deposition remains predominant in case of flowing. Moreover, they add that plugging mechanism occurs under certain conditions.

It must be noted that Wang and Civan are one of the pioneers of computational model about asphaltenes deposition. Their original model is the basis for most of the work done afterwards by numerous authors including themselves through different modified and improved versions of it. Wang and Civan (2001) established a model that simulate the asphaltenes precipitation and deposition in petroleum reservoir. To do so, they used a mass balance equation associated with precipitation, deposition, porosity and permeability reduction models into a three-dimensional black oil simulator. The model was verified with experimental data.

Minssieux et al. (1997) assimilate the asphaltenes deposition as fines particles migration damaging the reservoir. Doing so they successfully modeled the pore blocking mechanism and applied it to their experimental results.

Cruz et al. (2009) in their experimental study previously described in the last section, effectuate a modeling approach. They established and validated a mathematical model based on transport of stable particulate suspension. They used their experimental results as well as results from literature. They distinguish two mechanisms: adsorption and trapping as a result of asphaltenes deposition.

Behbahani et al. (2012; 2013; 2014) in their different study proposed a model based on multilayer theory equilibrium mechanism and four material balance equations. They test them with experimental results in the literature. They concluded their model is more accurate than those obtained from Wang and Civan's model based on the mechanical plugging mechanism, or the Langmuir equation.

2.4. Asphaltenes mitigation

2.4.1. Steam treatment

In their investigation described earlier, Zekri and Almehaideb (2001) did a trial treatment with steam. They concluded that steam may be applied as a treatment for the deposition of asphaltene in carbonate reservoirs. The steam treatment on average resulted in 94% of improvement in the permeability impairment.

2.4.2. chemical treatments

2.4.2.1. Treatment with xylene and bio-oil dispersant

This is a short description about some mitigations trial of asphaltenes deposition using chemicals products.

Sanada and Miyagawa (2006) worked on a case study of asphaltenes damaging the productivity of a field. Based on their laboratory analyses and tests, they designed a complete chemical treatment consisting of the injection of xylene in the formation with a three feet treatment radius. Their method resulted in a major improvement in the production as they were able to produce as much as ten time than before.

Alrashidi et al. (2018) investigate the mitigation of asphaltenes sludge by using dispersants during an acidizing treatment process. The core is a limestone, and they used coconut oil as a bio-oil dispersant. The results after their flooding indicate that using dispersant allows the reduction of the asphaltene sludge and produce better acid propagation through the core sample.

Using automated microfluidic devices, Chen et al. (2019) also added xylene as treatment to study the deposition of asphaltenes. They conclude that xylenes were more prone to dissociate asphaltenes deposited at a higher temperature than the ones at lower temperatures.

2.4.2.2. Treatments with non-ionic and acid surfactant

It is suggested that stabilization of asphaltenes can be affected by adding aromatic solvents such as toluene, benzene and xylene, which can aid in stabilizing the asphaltene micelles and inhibit the precipitation process. The stability of micelles can be enhanced by the introduction of compounds of similar nature to resin. Compounds that have a polar head containing an acidic group which can attach to the micellar core. These chemicals can be natural resins extracted from crude oil or oil-soluble amphiphiles (Al-Sahhaf et al., 2001).

Surfactant is a chemical used in the industry for generally enhanced oil recovery operations. We do know also they have some similitudes with the resins in crude oil. Surfactants are usually organic compounds that are amphiphilic, meaning they contain both hydrophobic groups (their tails) and hydrophilic groups (their heads).

Hashmi and Firoozabadi (2013) study the mitigation of asphaltenes deposition using different surfactants. They used a lab scale metal pipe, induce precipitation of asphaltenes in it by use of n-heptane as precipitant. They end up assessing the inhibition or reversal of the deposition by using separately different chemicals as treatments. They used 0, 1, 2, 100 GPT of non-ionic surfactant and 5 GPT of strong acid surfactant: dodecyl benzene sulfonic acid (DBSA). They found out the nonionic surfactant can stabilize the asphaltenes deposition. While the best results are found with

the DBSA that was able to effectively remove asphaltene deposits quickly and at lower concentrations than required by toluene.

CHAPTER 3: EXPERIMENTAL METHODS

This chapter presents the various experimental methods used to characterize the core plug and crude oil used during our investigations as well as a description of the experimental apparatus used to evaluate asphaltenes accumulations in the core plug.

3.1. Fourier transform infrared method for quantification of mineralogy

Transmission FTIR was used to quantify the mineralogy of the core sample used during the present study. During FTIR measurements, a pellet constituted of rock sample potassium bromide (KBr) is exposed to a polychromatic light source. A detector located after the sample measures the amount of energy lost at different frequencies due to the vibration of the molecular bonds present in the sample. This energy loss as function of frequency quantified as absorbance is dependent on the type of minerals present in the sample, their amounts, and the thickness of the sample. The relationship between the absorbance at a given frequency and the concentration of a given mineral is materialized by Beer's Law:

$$A_v = \sum_{i=1}^{n} \varepsilon_i l c_i \qquad (1)$$

Where A_v is the absorbance at a given frequency, ε_i is the absorptivity of the mineral, l is the optical path length and c_i is the concentration of the mineral. FTIR is a true quantitative method, unlike X-ray diffraction which is a semi-quantitative. Computation of mineral concentrations using Beer's Law requires a library of the spectra of the minerals of interest at various

concentrations (Sondergeld and Rai 1993; Ballard, 2007). Examples of such spectra are presented in Figure 3.1.
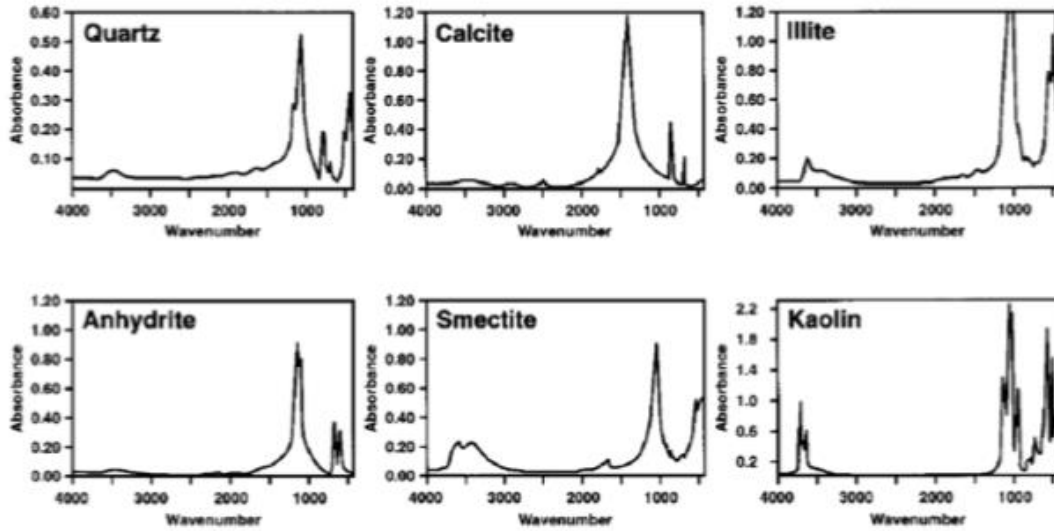
Figure 3.1. Examples of FTIR spectrum of quartz, calcite, illite, anhydride, smectite kaolinite (Sondergeld and Rai, 1993).

3.2. Soxhlet extraction method

Soxhlet extraction is an experimental procedure that we have during the sample preparation before every experiment. A Soxhlet extraction apparatus is constituted of a flask containing a solvent connected to an extraction chamber with a condenser on top (Figure 3.2).
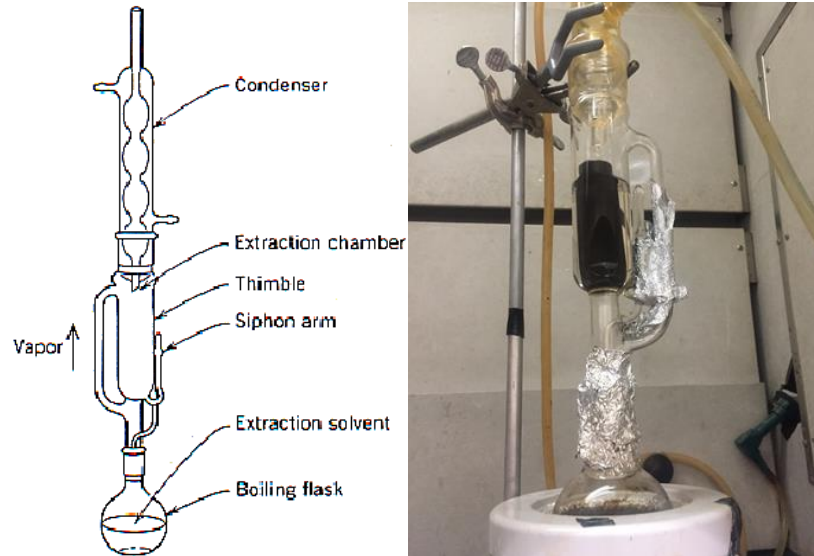
Figure 3.2. Schematic and picture of the Soxhlet extraction apparatus.

The extraction chamber contains a siphon that allows solvent refluxing during the extraction process. Our Soxhlet extractions were conducted with dichloromethane at 122°F. Dichloromethane was used during this study because it could dissolve in the sample pores all the oil components.

3.3. Mercury intrusion capillary pressure (MICP) measurements

MICP measurements were used to determine the pore throat size distribution of the core sample. MICP measurement consists of quantifying the volume of mercury injected in a sample at different pressure steps. To start our MICP measurements the Soxhlet extracted and dried sample is placed in a penetrometer which is a glass cylinder connected to a hollow stem. The penetrometer containing the sample is subsequently introduced in a Micrometrics Autopore IV™ (Figure 3.3) where mercury is injected into the sample via the penetrometer stem.

Figure 3.3. Micrometrics Autopore IV™ located in the Integrated Core Characterization Center of the University of Oklahoma.

The maximum injection pressure that the Autopore IV™ can achieve is 60,000 psi. Using the Washburn equation (equation 2) each mercury intrusion pressure can be converted into a pore throat radius.

$$r = \frac{2\gamma \cos(\theta)}{P_{Hg}}$$
(2)

In Equation 2, r is the pore throat radius (cm), PHg is the mercury intrusion pressure in dyne/cm2, γ is the interfacial tension (dyne/cm) for the system air-Hg (480 dyne/cm), and Θ is the contact angle (140°). Using the Washburn equation, the smallest throat radius measurable with the MICP method is 1.5 nm.

3.4. Brine saturation method

The core sample was saturated with brine before every asphaltenes accumulation experiment. Prior to brine saturation, the Soxhlet extracted sample is inserted in a hydrostatic pressure vessel (Figure 3.4) where it is subjected to vacuum for 30 minutes. After the sample is evacuated, a valve leading to a brine container is opened to allow the entry of brine in the pressure vessel. When the pressure vessel is filled, 2,000 psi of brine hydrostatic pressure is applied to the sample for 24 hours.
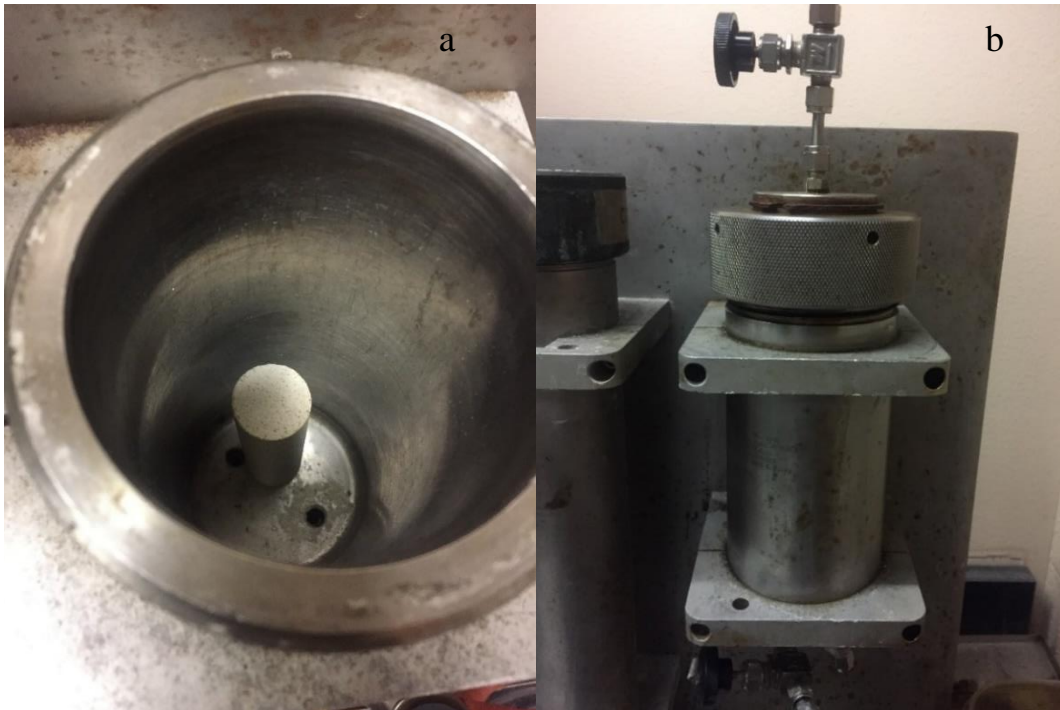
Figure 3.4. Picture of (a) the core sample inside the saturation core vessel; (b) the set hermetically closed for vacuum then brine saturation.

3.5. Permeability measurement

The absolute permeability of the core plug was determined with the steady state method. The Soxhlet extracted and dried sample was inserted in hassler sleeve that was introduced in a hydrostatic core holder connected to a syringe pump containing crude oil. To determine permeability crude oil was flown through the sample at a constant flowrate of 0.025 ml/min while the outlet was maintained at atmospheric pressures.

3.6. Quantification of crude oil asphaltenes content

A modified version of the ASTM 2007-80 method was used to quantify the asphaltene content of the crude oil. 80 ml of n-heptane was added to 2g of crude oil to induce asphaltenes precipitation. The mixture of n-heptane- and crude oil is stirred and allowed to rest for 48 hours before filtration. The filter paper used is an EMD Millipore 0.22 µm size filter. Before filtration, the filter paper is dried at 225 °F for 15 minutes and allowed to cool to room temperature in a desiccator. The assembly used for filtration has a funnel with a sintered disk as a base, a clamp and a vacuum flask (Figure 3.5).

Figure 3.5. Picture of the assembly used for asphaltenes quantification.

The mass percentage of asphaltenes in the crude oil sample is determined by equation 3.

$$A_C = \frac{A_m}{O_m} \times 100 \tag{3}$$

Where A_c is the mass percent of asphaltenes (%), A_m is the asphaltenes mass (g) and o_m is the crude oil mass (g).

3.7. Quantification of crude oil sediment content

Sediment content was quantified in the crude oil. 10 ml of the crude is mixed with 100 ml of toluene. The toluene is used to dissolve any organic content and wax in the crude. The mixture is heated and stirred for 15 minutes at 194°F. The mixture is then filtered using the same process and apparatus as the asphaltene quantification previously described.

3.8. Measurement of crude oil viscosity and density as function of temperature

Viscosity and density of the crude oil are measured at various temperatures. The viscosity was determined by introducing 60 ml of the crude in a rotary capillary/Ostwald Viscometer and automatically heated gradually. The density of crude oil was determined with a glass pycnometer which was heated to several temperatures in a water bath.

3.9. Minimum miscibility pressure (MMP) measurements

MMP is the smallest pressure at which two fluids are miscible. To measure MMP between the crude oil and the gas mixture (72% methane and 28% ethane), we have used the vanishing interfacial tension (VIT) method (Hawthorn et al., 2016). This method considers that the MMP is the pressure at which the interfacial tension between two fluids is equal to zero. To implement the VIT method, we have the experimental apparatus developed by Mukherjee (2020) (Figure 3.6).
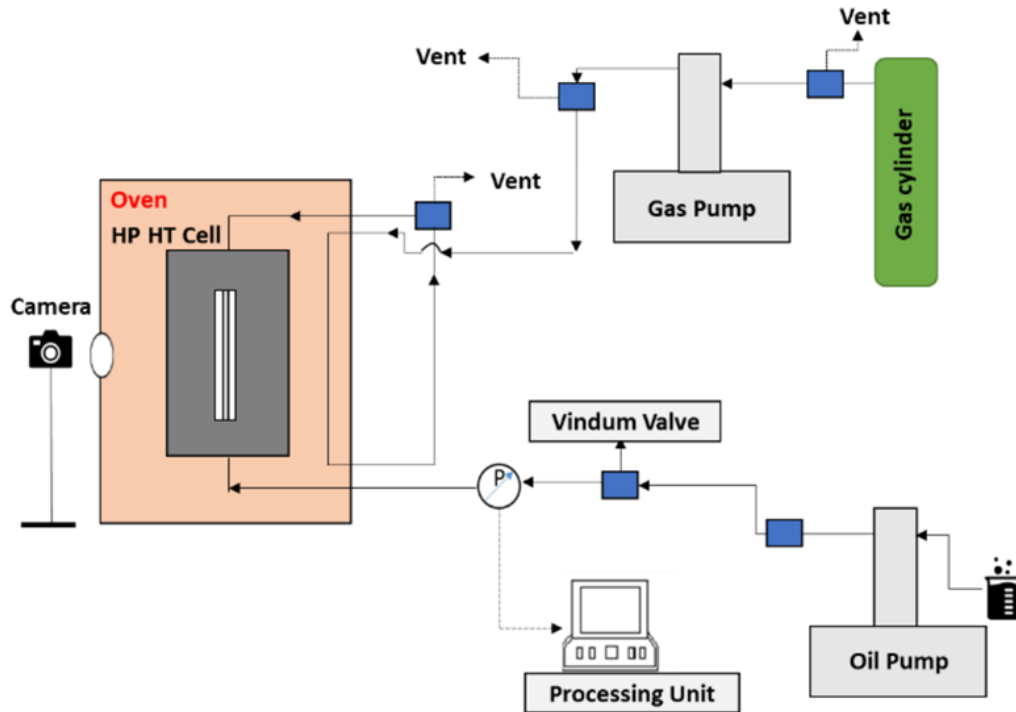
Figure 3.6. Experimental apparatus used for the VIT MMP measurements (Mukherjee, 2020). The HP-HT cell is equipped with a sapphire window that allows the visualization of the crude oil and gas interactions.

To start the measurement, a glass capillary tube with a diameter of 0.6 mm is placed in the high pressure-high temperature (HP-HT) cell containing oil such that capillary rise can be observed. The following step is to use the gas pump to add the gas mixture in the HP-HT cell at different pressures. The pressure at which we cannot observe a capillary rise is the MMP.

3.10. Contact angle measurement

Contact angle measurements were used to evaluate the wettability of the core before and after preparation. To measure the contact angle, we have used the Kruss Easy Drop goniometer.
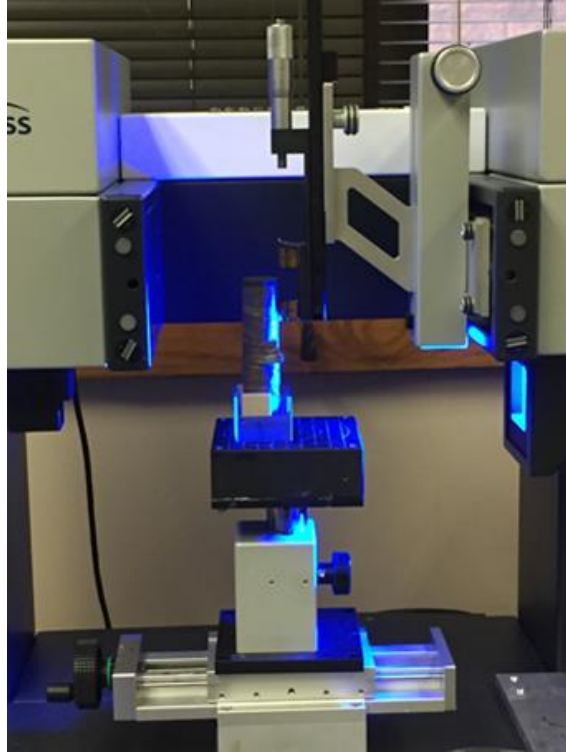
Figure 3. 7. Picture of the contact angle measurement apparatus.

The contact angle measurements were conducted between the core sample and an oil droplet when the core sample was immersed in brine.

3.11. Description of the apparatus used for oil and gas injection

To study the phenomenon of asphaltenes accumulation in porous media during oil and gas flow we have designed and assembled a unique experimental apparatus that allows the co-injection of oil and gas. Figure 3.8 presents a picture of the apparatus while Figure 3.9 illustrates a schematic of the apparatus. All valves and pumps of this apparatus can be controlled by a software constructed in Labview.

Figure 3.8: Picture of the apparatus used for the co-injection of oil and gas.
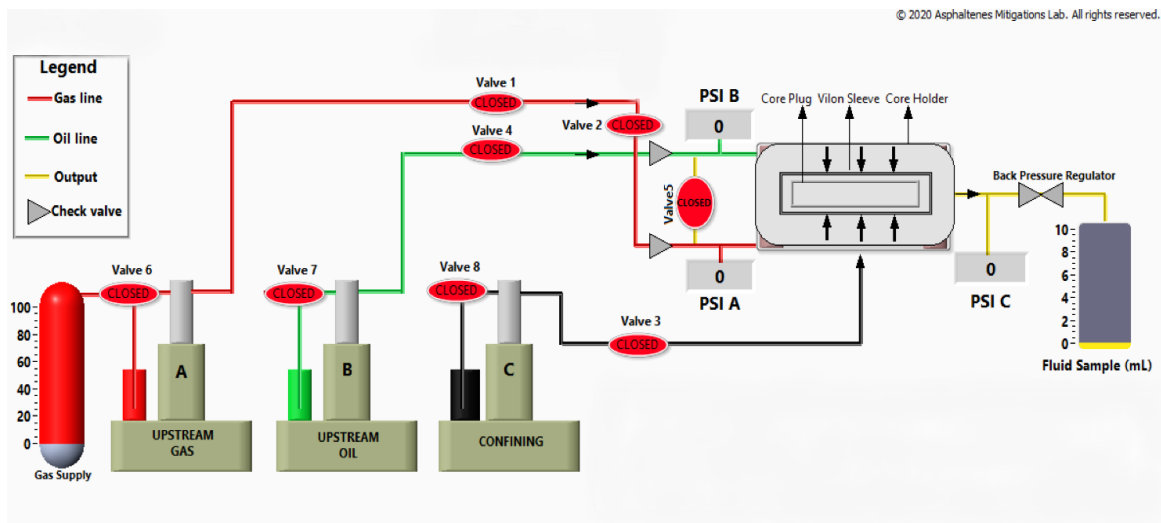
Figure 3. 9. Schematic of the apparatus used for co-injection of oil and gas.

The apparatus is constituted of three syringe pumps that are used for oil and gas injection as well as to apply the confining pressure independently. The oil and gas pumps are connected to the core holder injection ports by high-pressure stainless-steel lines equipped with check-valves that prevent flow back into the pumps. A backpressure valve placed on the outlet side of the core holder is used to control the pore pressure during the experiments. Two Pressures transducers are placed before the gas and oil injection ports and a third one is between the outlet port and the backpressure regulator. These pressure transducers are used to record the pressures at the entrance and exit of our core sample.

The core holder is equipped with 2 independent injection ports for oil and gas (Figure 3.10). A thin Teflon wafer is inserted between the injection ports and the core sample to prevent oil and gas from mixing at the core face (Figure 3.11).
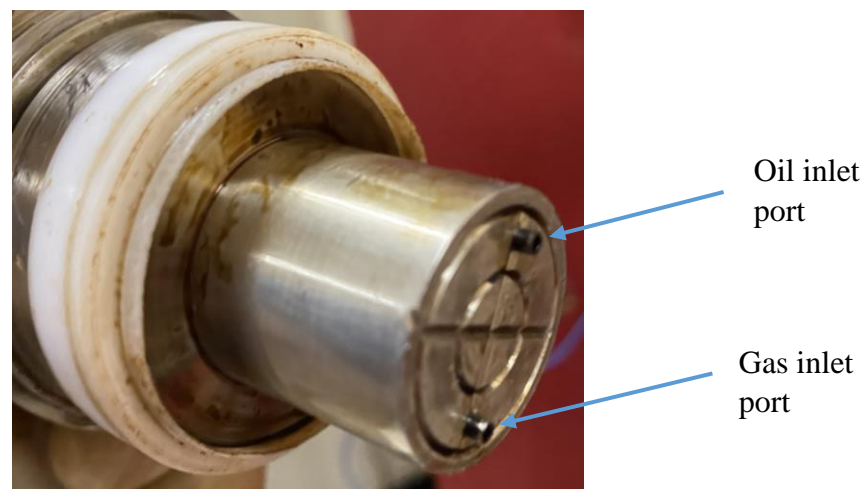
Figure 3.10. Oil and Gas inlet ports. The injection ports are extended in order to allow the placement of a thin Teflon wafer
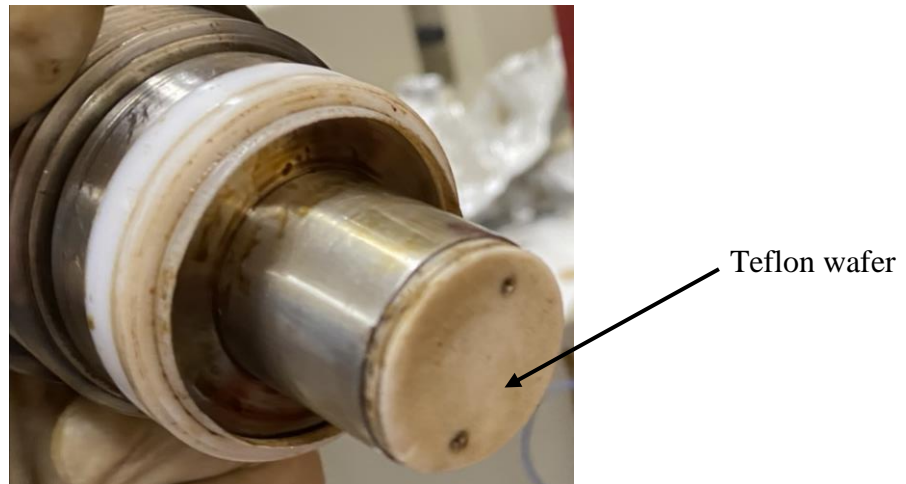
Figure 3.11. Teflon wafer used to isolate the oil and gas injection ports

To ensure that the oil and gas will not mix on the core face, we evaluated the communication level between the two injection ports. This evaluation was conducted with a solid aluminum plug inserted in the core holder and an injection of nitrogen at 4,500 psi during 16 hours. The backpressure was kept at 4,500 psi during this test. Figur 3.12 presents the pressures recorded at the gas inlet, oil inlet and outlet of the sample. During the 16 hours, the pressure at the oil inlet and gas inlet remained constant at 7 ± 3 psi. Therefore, the communication between the two injection ports is minimal.
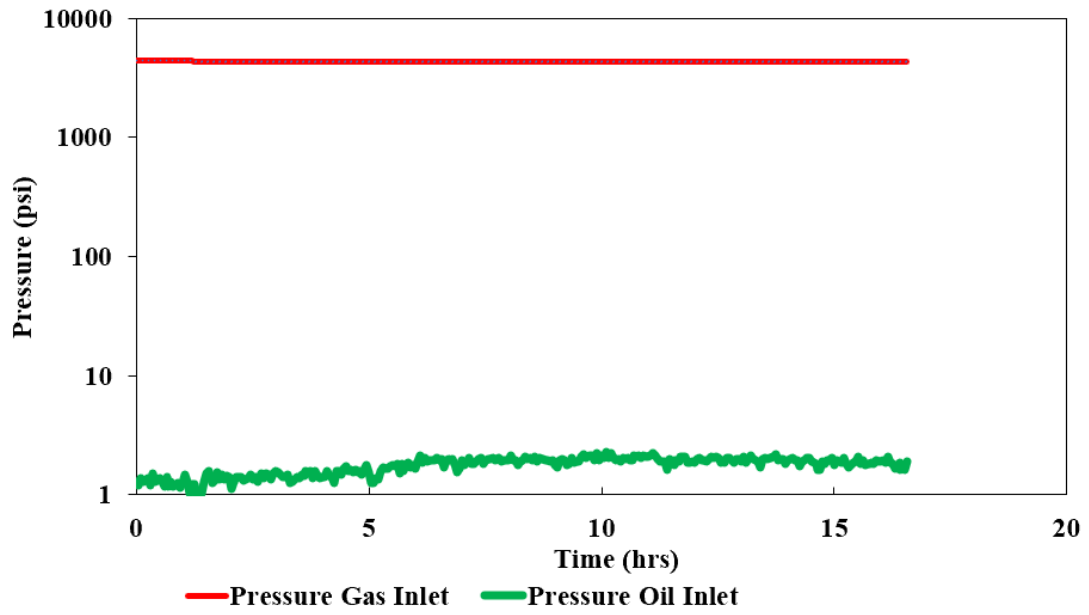
Figure 3.12. Pressures recorded at the oil inlet, gas inlet and outlet of the core during the evaluation of the communication between the injection ports.

CHAPTER 4: EXPRIMENTAL RESULTS AND DISCUSSION

4.1. Core characterization

For the purpose of this project study, we have used a Berea sandstone core plug with length and diameter equal to 9.32 cm and 2.51 cm respectively (Figure 4.1). A single core plug was used throughout this study in order to limit the variability of experimental results due to heterogeneity between different samples.

Figure 4.1. Picture of the Berea sandstone core plug used for the experiments.

FTIR mineralogy measurements indicate that the Berea sample had 81% of quartz, 6.7% of clay and minor amounts of dolomite. Porosity value of 20.4% was computed from the weight

difference before and after saturation with 35 g/l brine while the steady state permeability measurements yielded 16 mD at an effective stress of 1,000 psi.

MICP measurements show that the main pore throat size radius is 39.96 µm while the average pore size diameter is 3.66 µm (Figure 4.2).
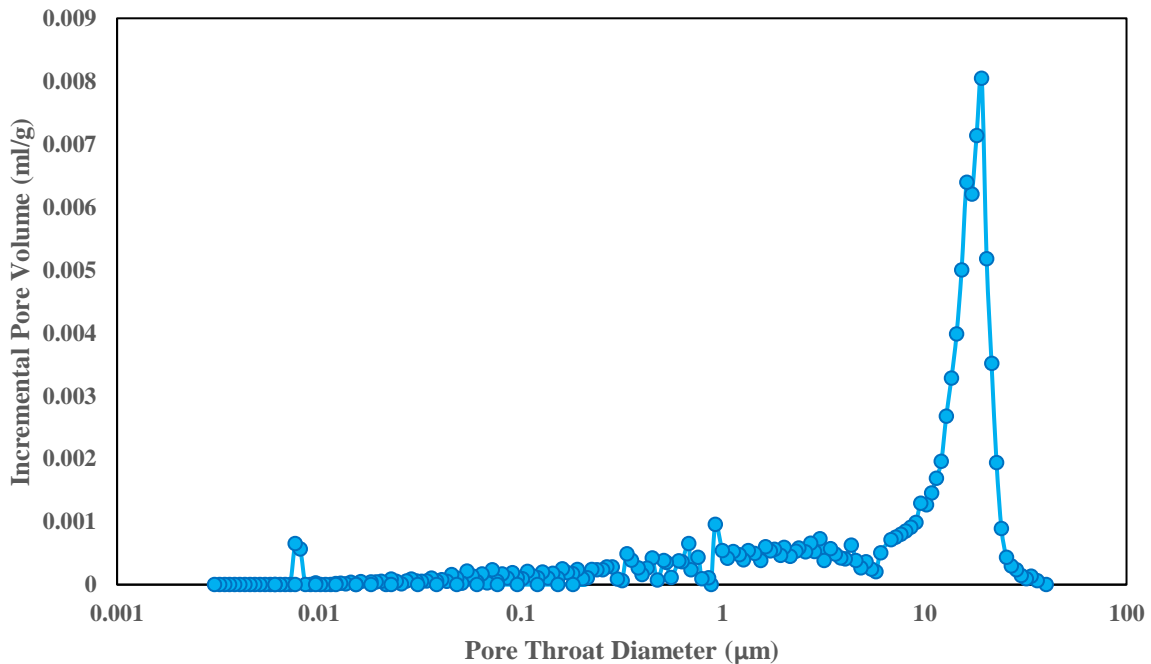
Figure 4.2. MICP pore throat size distribution of the Berea sample.

4.2. Crude oil characterization

Upon reception, the crude oil used in our investigation has 1.05 wt% of solid content. Such amount of solid content was large enough to prevent oil flow within the core sample. Therefore, the crude oil was filtrated with a sintered disk with 0.5 µm mesh size. The filtered crude oil had 0.1 wt% of solid content and 4.04 wt% of asphaltenes content.

The sintered disc size was selected because of the pressure used for the oil filtration (3,000 psi). However we used 0.5 µm of filter size which could affect the results because the average pore size distribution diameter of the core sample is 3.66 µm. Pores throat diameter smaller than 0.5 µm could be plugged by sediments.

Figure 4.3 and Figure 4.4 present the crude viscosity and density measurements repectively. They indicate that the oil viscosity varies from 19.2 to 6.38 cp and the density changes from 0.89 to 0.84 g/cc when the temperature increases from 86 to 176 °F.
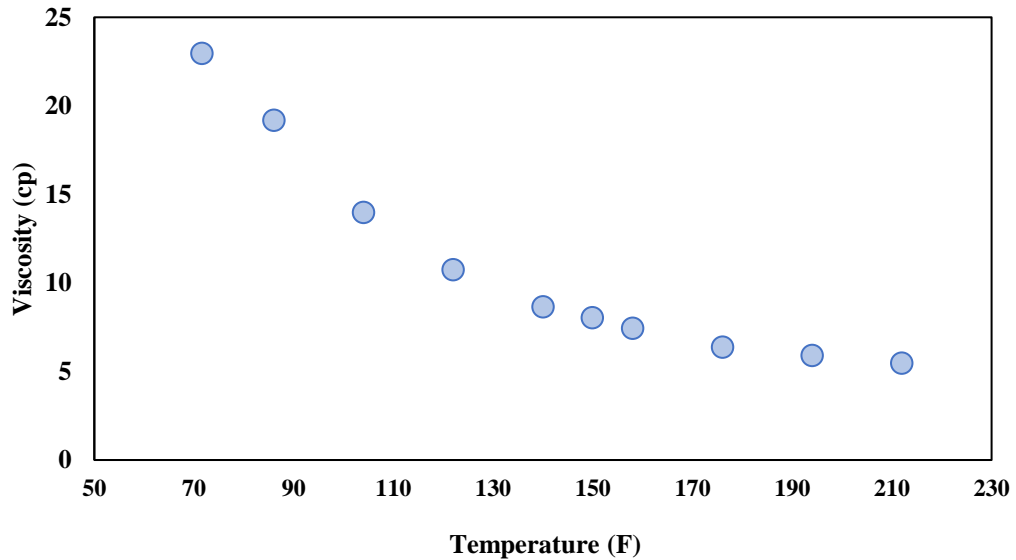
Figure 4.3. Viscosity of the crude oil as function of temperature.
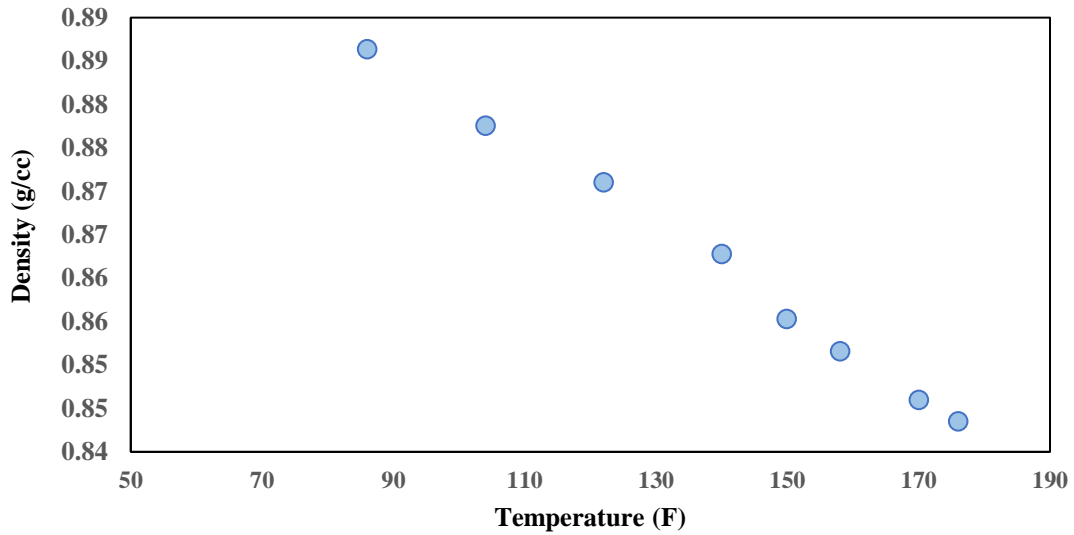
Figure 4.4. Density of the crude oil as function of temperature.

MMP measurements with the vanishing interfacial tension method yielded 4,200 psi between the crude oil and the gas mixture (72% methane-28% ethane).

4.3. Investigation of impact of pressures and flowrates on asphaltenes accumulation

4.3.1. Sample preparation

Before each experiment, the Berea sample was saturated with a 35 g/l brine. The brine saturation is subsequently reduced to irreducible water saturation (S_{wir}) by the injection of crude oil at a flowrate of 0.025 ml/min, constant pressure of 4,500 psi and a temperature of 170° F. 4 to 6 pore volumes (PV) of crude oil injection were necessary to reach S_{wir} (Figure 4.5). Figure 4.6 shows that S_{wir} ranges between 29.6 and 34.96% prior to the investigations of the impact of pressure and flowrate on asphaltenes accumulation.
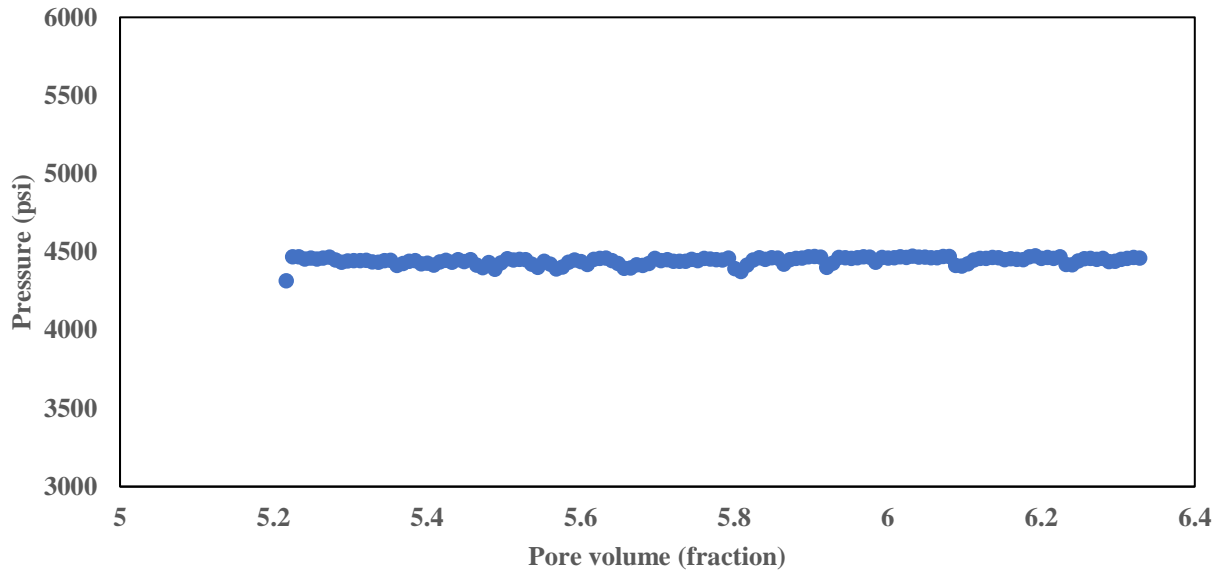
Figure 4.5. Pressures recorded at the oil inlet of the core sample as function of pore volume with a backpressure equal to 4,500 psi (1.07% MMP) and flowrate of 0.025 ml/min.
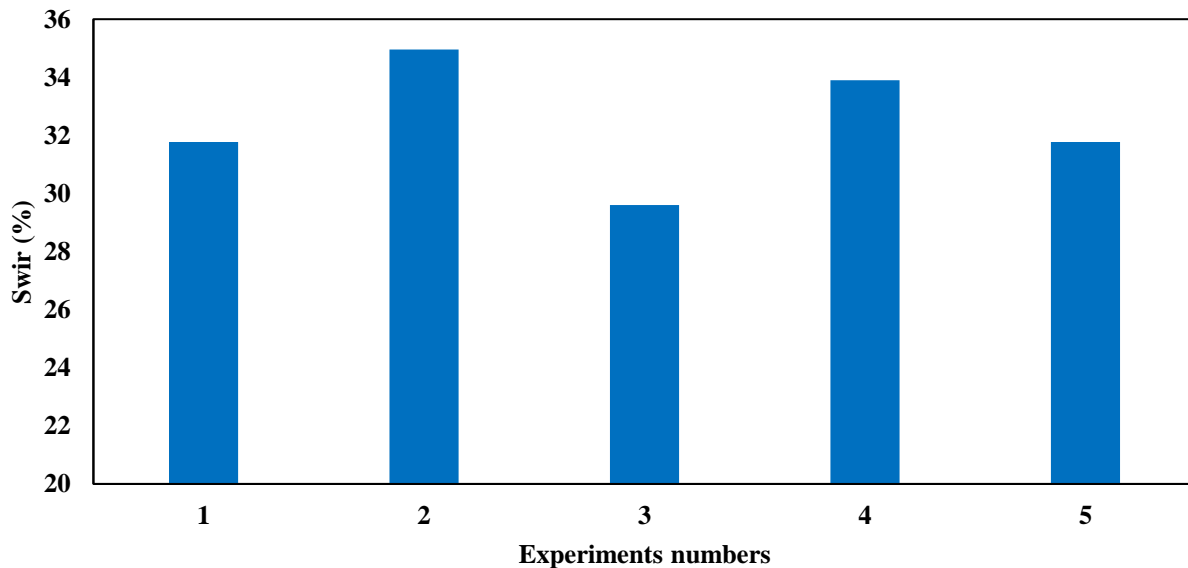
Figure 4.6. S_{wir} values obtained prior to the experiments investigating the impact of pressure (1,2,3) and flowrate (4,5) on asphaltene accumulation. An average S_{wir} of 32.4% ± 2.6 was obtained prior to these experiments.

After the establishment of S_{wir}, crude oil was maintained in the core sample at 4,500 psi of pore pressure (5,800 psi of confining pressure) for 7 days. This aging process was followed to alter the wettability of the Berea core plug toward oil wetness. The wettability of the core plug was assessed with contact angle measurements. Figure 4.7 shows the pictures of oil droplets in contact with the core sample after saturation with brine (35 g/l NaCl) where a contact angle close to 11° was measured.
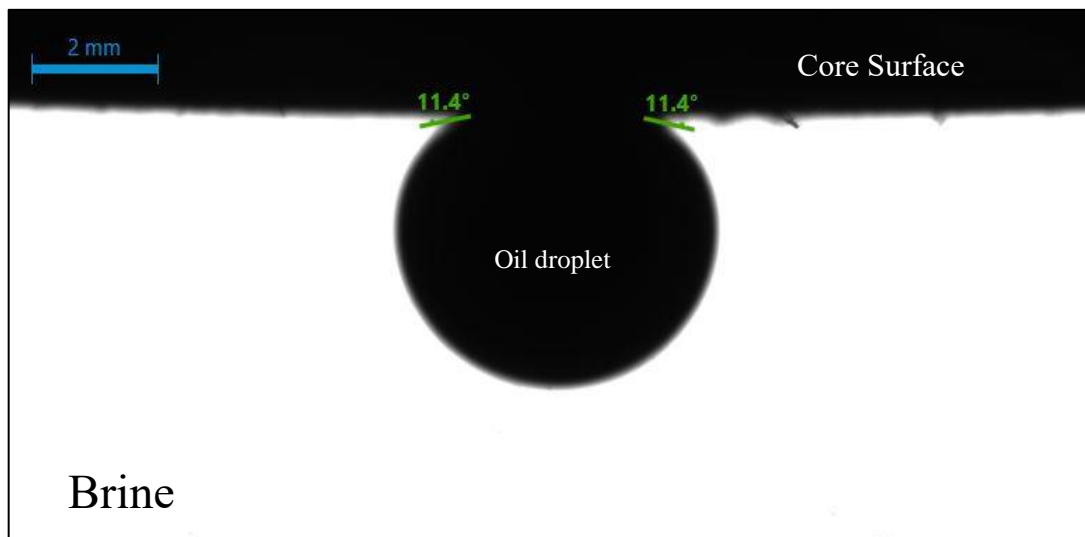
Figure 4.7. Contact angle measurement between an oil droplet and the Berea core plug saturated with brine.

The contact angle measurement conducted after the aging step is illustrated in Figure 4.8. After aging, the contact angle between the oil droplet and the core sample increased to 130° indicating that the aging process has successfully altered the wettability of the core sample to oil wet.
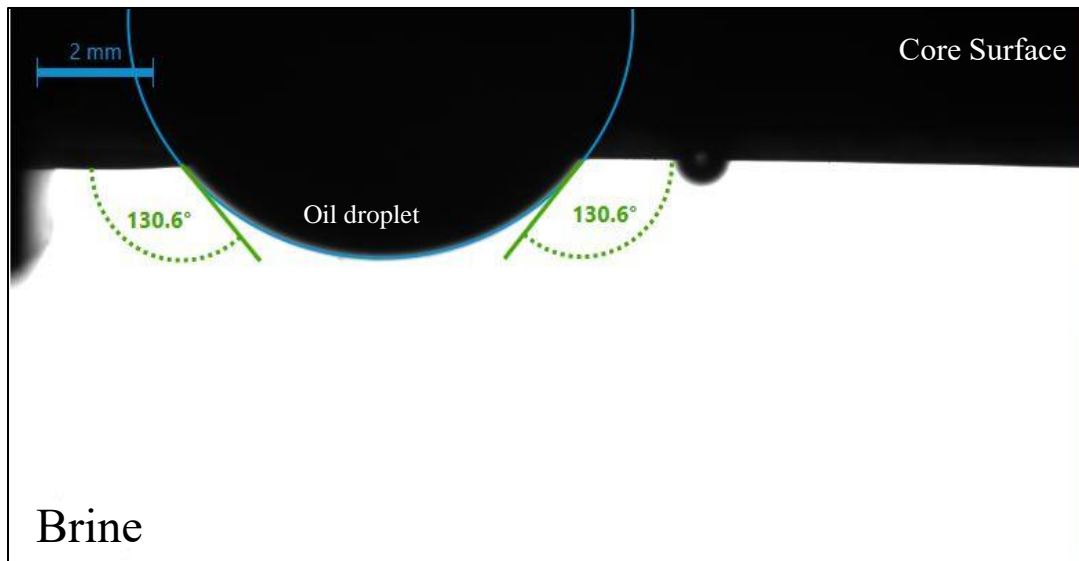
Figure 4.8. Post aging contact angle measurement between an oil droplet and the core plug initially saturated with brine.

4.3.2. Results of the impact of pressure on asphaltene accumulation

To evaluate the impact of pressure on asphaltenes accumulation in porous media, we conducted three gas and oil co-injection experiments at 4,500, 3,570 and 3,150 psi of backpressures with a constant flowrate of 0.025 ml/min and a temperature of 170°F. These pressures that represent 1.07, 0.85 and 0.75% of the MMP were selected in order to compare asphaltenes accumulations close to the MMP and below the MMP.

As indicated previously, the MMP between the crude oil and the n-alkane gas mixture (72% methane+28% ethane) is 4,200 psi.

The Reynold number for these experiments was 0.011. The core sample diameter was used for the computation.

Instead of mixing of the oil and gas in a pressure vessel we conducted a co-injection of oil and gas in the sample in order to prevent the asphaltenes precipitation prior to core flooding.

Figure 4.9 presents the recorded pressures at the oil and gas inlets as well as at the core outlet during the experiment at 1.07 % of MMP. We observe an initial transient period in which the injection pressures are initially relatively constant (4,450 psi ± 50) up to 4.5 pore volumes where we observe a sudden increase in the oil and gas inlet pressures.
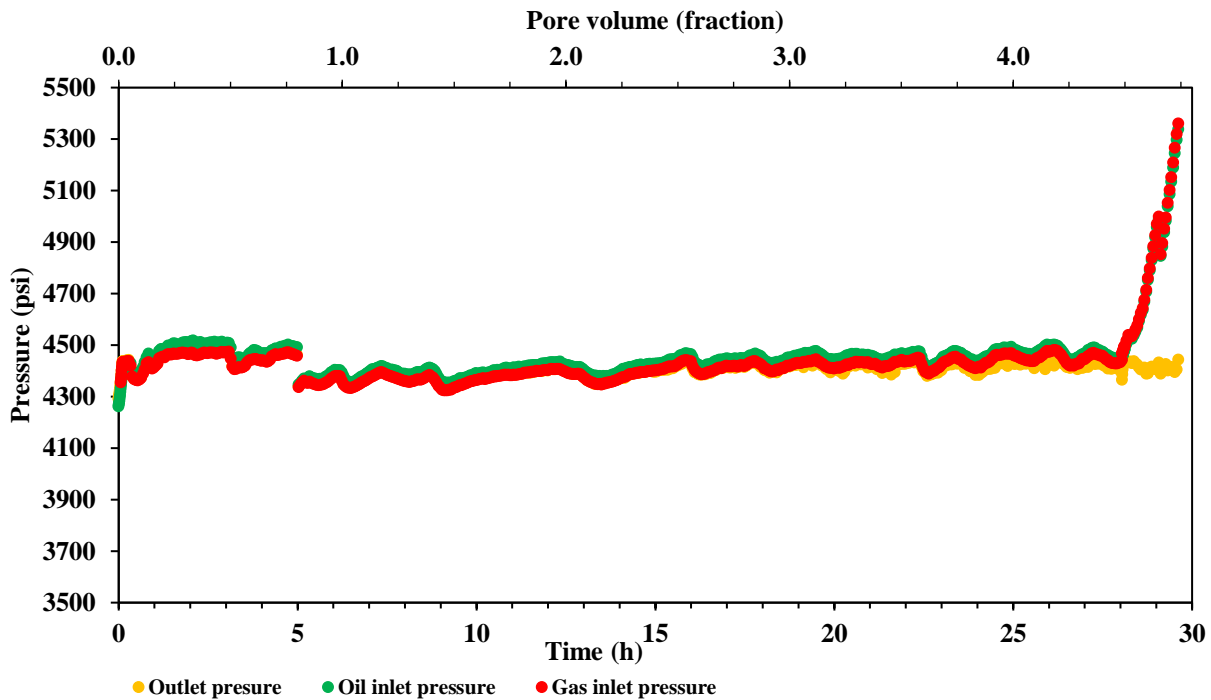
Figure 4.9. Pressures recorded at the oil inlet, gas inlet and outlet of the core sample as function of time and pore volume with a backpressure equal to 4,500 psi (1.07% MMP).

The injection was stopped after the pressures reached 5,400 psi in order to not exceed the pressure limitations of the apparatus. This increase in pressure indicates a permeability impairment due to asphaltene accumulation in the core sample.

A plot of the pressure drops across the sample (Figure 4.10) also implies a severe obstruction of the flow path after the injection of 4.5 pore volumes. We observe a difference in the oil and gas pressure drop from the beginning of the experiment up to 3.7 PV. This difference in pressure drops

43

could be due to the fact that these experiments were conducted at constant injection rates instead of constant injection pressures. Therefore, the viscosity and permeability may be different for both fluids at that point. This is valable for all experiments where we observe difference in oil and gas pressure drops.
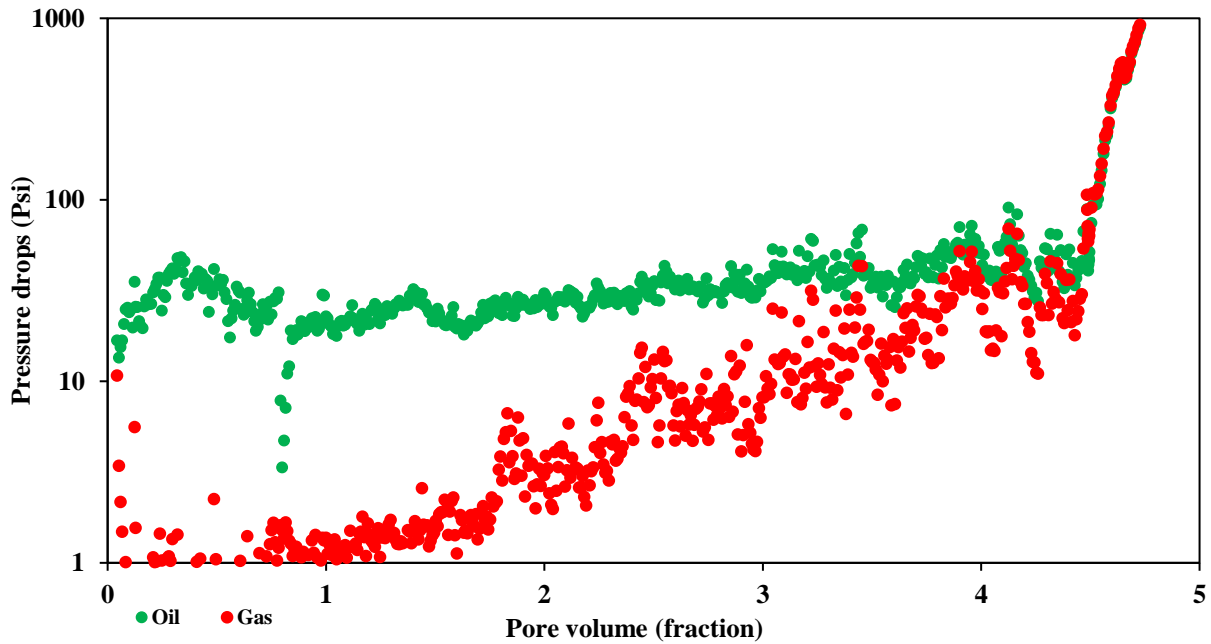
**Figure 4.10. Pressure drops recorded of oil and gas across the sample as function of pore volume with a backpressure equal to 4,500 psi (1.07% MMP).**

A major concern of experimental study on formation damage due to asphaltenes accumulations is the mixing of oil and gas at the core face, hence the asphaltenes accumulation is concentrated at the core face. However, the Teflon wafer we designed and manufactured, prevented oil and gas from mixing at the core face. Figure 4.11 shows a color change in the core sample indicating that asphaltene deposition started close to 2.5 cm away from the inlet core face. Therefore, the results of the present study are representatives of a deposition process taking place within the core sample and not on the core face.
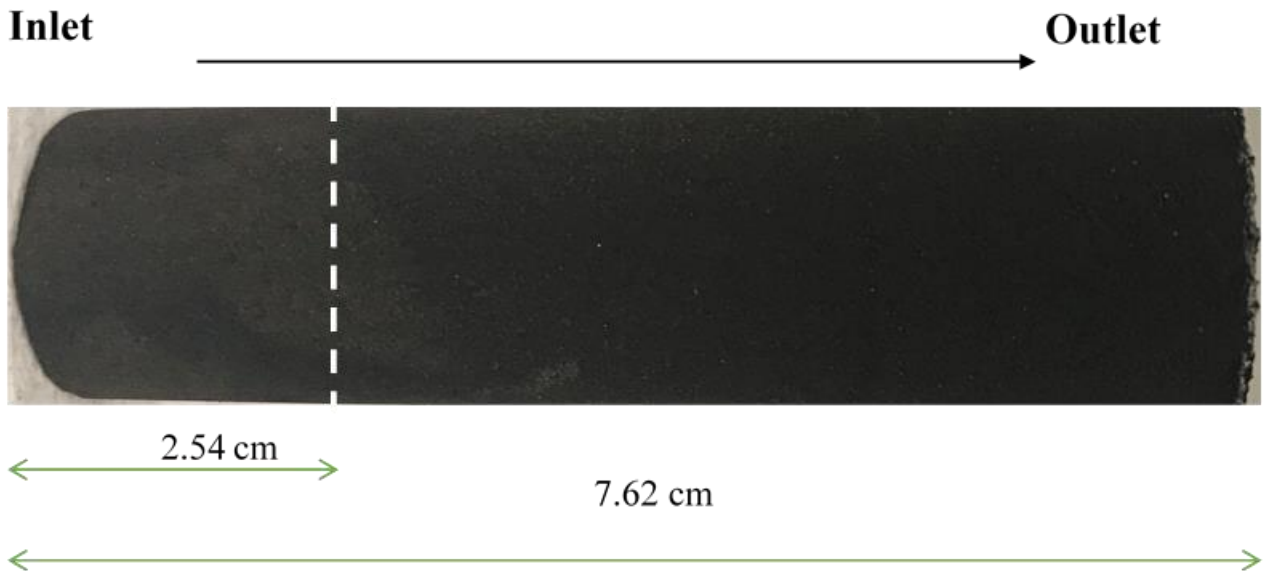
Figure 4.11. Picture of the Berea sandstone core plug after the co-injection of oil and gas (72% C1 and 28% C2). The color change at 2. 5 cm from the inlet indicates that the formation damage has occurred within the core plug and not at the core face.

During the experiment conducted at 3,570 psi (0.85% of MMP) the oil and gas inlet pressures were constant at $3,600 \pm 20$ psi until approximately 6.5 pore volumes where we observe a gradual increase in the oil and gas inlet pressures (Figure 4.12). These pressures reached a maximum of 4,000 psi at 7.75 pore volumes before decreasing. The plot of the oil and gas pressure drops associated with this experiment confirms the existence of formation damage due to asphaltenes accumulation after the injection of 6.5 pore volumes (Figure 4.13). However, the reduction of the oil and gas pressure drop across the sample after the injection of 8.5 pore volumes indicates the removal of the asphaltene previously accumulated in the core sample. This removal can be due to a redissolution of the asphaltenes in the crude oil due to the lower solubility of the gas mixture below the MMP value.
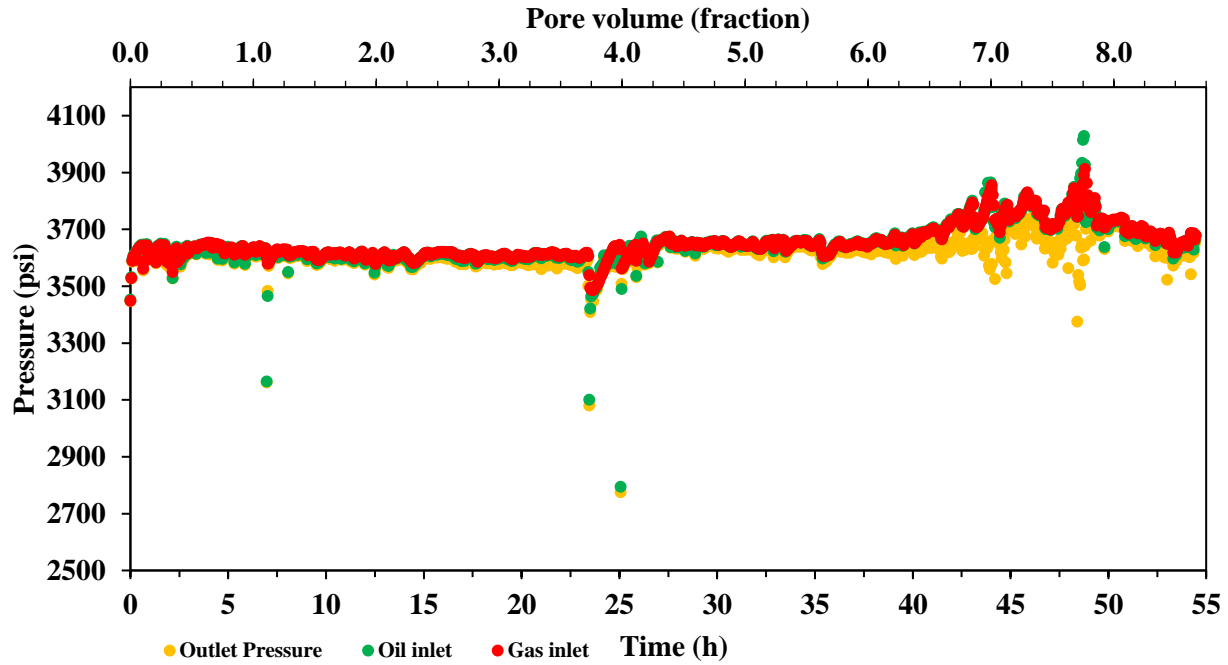
Figure 4.12. Pressures recorded at the oil inlet, gas inlet and outlet of the core sample as function of time and pore volume with a backpressure equal to 3,570 psi (0.85% MMP).

Figure 4.13. Pressure drops recorded for oil and gas across the sample as function of pore volume with a backpressure equal to 3,570 psi (0.85% of MMP).

At 3,150 psi (0.75% of MMP) of backpressure, we observe a reduction in the oil inlet, gas inlet and outlet after the injection of 1.25 pore volumes until 1.7 pore volumes. This pressure reduction could be due to a temporary backpressure failure. However, this possible temporary failure seems to be resolved after 1.75 pore volumes. After the co-injection of 6.5 pore volumes, we observe an increase in the oil inlet, gas inlet and outlet pressures (Figure 4.14). The plot of oil and gas pressure drops across the core sample shows a permeability impairment due to asphaltenes accumulation (Figure 4.15).

Figure 4.14. Pressures recorded at the oil inlet, gas inlet and outlet of the core sample as function of time and pore volume with a backpressure equal to 3,150 psi (0.75% MMP).
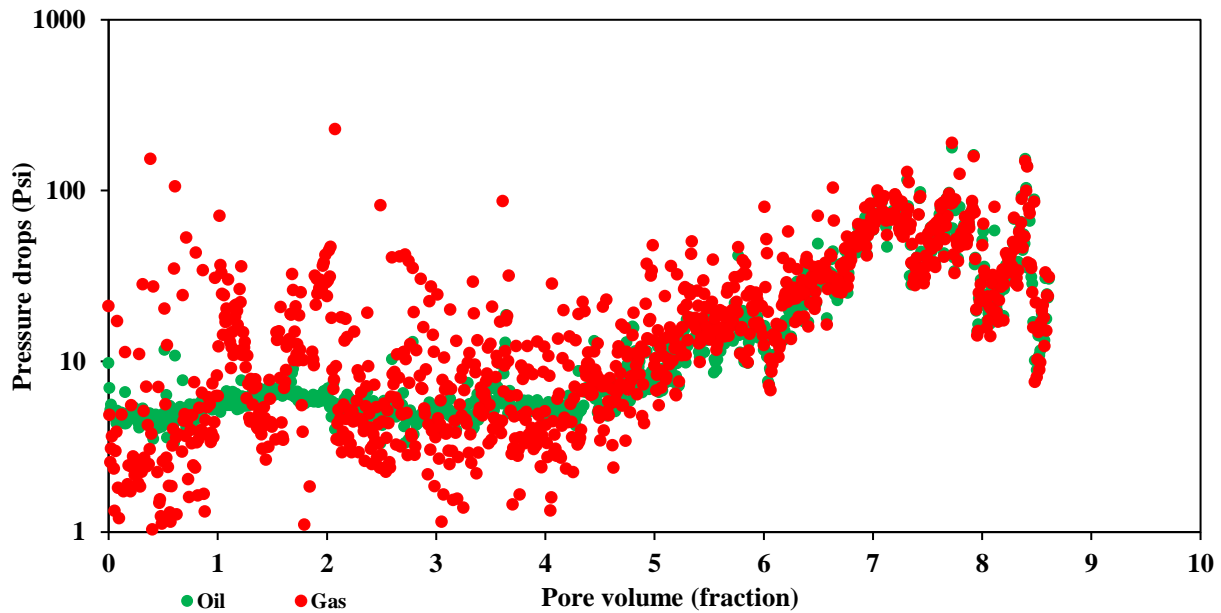
Figure 4.15. Pressure drops recorded for oil and gas across the sample as function of pore volume with a backpressure equal to 3,150 psi (0.75% of MMP).

Figure 4.16 presents a comparison of the gas pressure drop across the sample for the experiments investigating the impact of pressure on asphaltene accumulation at 4,500 psi, 3,570 psi and 3150 psi. Only the gas pressure was selected in this comparison because the oil and gas pressure drops were similar for these experiments. Figure 4.16 indicates that formation damage due to asphaltene accumulation is severe near the MMP but reduces significantly as the pressure reduces below the MMP due to the higher solubility of asphaltene in crude oil at lower pressures. The fact that at least 4.5 pore volumes injection is required, indicates that asphaltene accumulation will be important only in the near wellbore region and near the fracture face in hydraulically fractured wells.
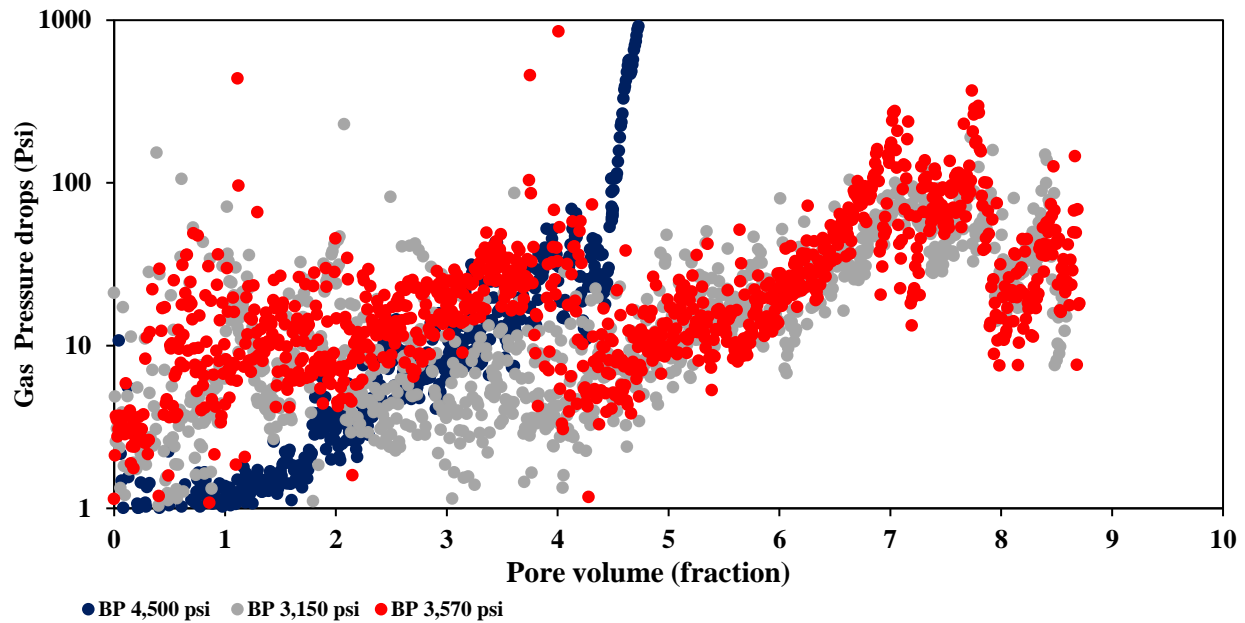
Figure 4.16. Comparison of pressure drop recorded for gas across the sample as function of pore volume with backpressures equal to 4,500, 3,570, 3,150 psi at a flowrate of 0.025ml/min.

4.3.3. Results of the impact of Flow rate on asphaltene accumulation

The impact of flowrate on asphaltenes accumulations in core samples was evaluated at 4,500 psi (1.07% of MMP) and 3.570 psi (0.85% of MMP) of backpressures. The experiments consisted in the co-injections of oil and gas (72% methane + 28% ethane) at flowrates of 0.025 ml/min and 0.25 ml/min at a constant temperature of 170°F and the pressures specified above. The Reynold number computed for both experiments was 0.11.

The results of the experiments conducted at a flowrate of 0.025ml/min have already been discussed in section 4.3 (Impact of pressures on asphaltene accumulation). At 0.025 ml/min we essentially observed at 4,500 psi (1.07% of MMP) significant increase in the oil and gas pressure drops

because of asphaltene accumulation. At 3,570 psi (0.85% of MMP) and 0.025 ml/min of flowrate the pressure drops of oil and gas experience a relatively small increase (400 psi) before returning to their baseline value indicating temporary formation damage.

At 0.25 ml/min of flowrate, the oil and gas inlet pressures are relatively constants (Figure 4.17 and Figure 4.18). Even after the injection of 8.5 to 9 pore volumes the plots of oil and gas pressure drops (Figure 4.19 and Figure 4.20) also do not show an increase in the pressure drops. Therefore, at 0.25 ml/min asphaltenes do not accumulate in the sample. The results of these experiments indicate formation damage due to asphaltenes accumulation can be avoided even near MMP by increasing flowrates (Figure 4.21 and Figure 4.22).
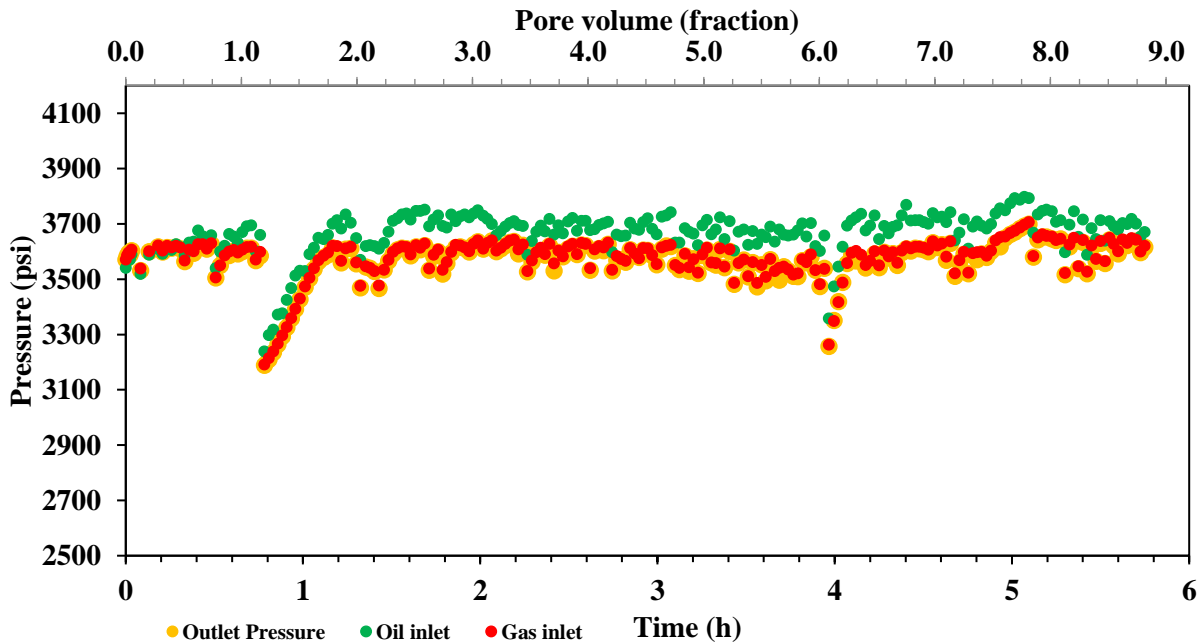
Figure 4.17. Pressures recorded at the oil inlet, gas inlet and outlet of the core sample as function of time and pore volume with a backpressure equal to 3,570 psi (0.85% MMP) at flow rate of 0.25 ml/min.
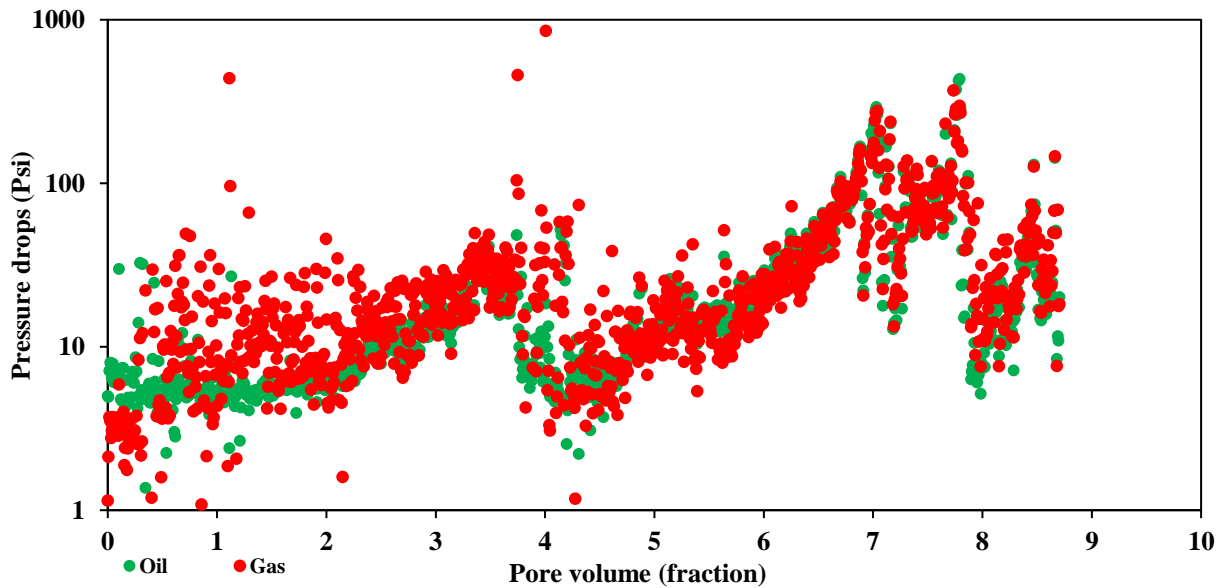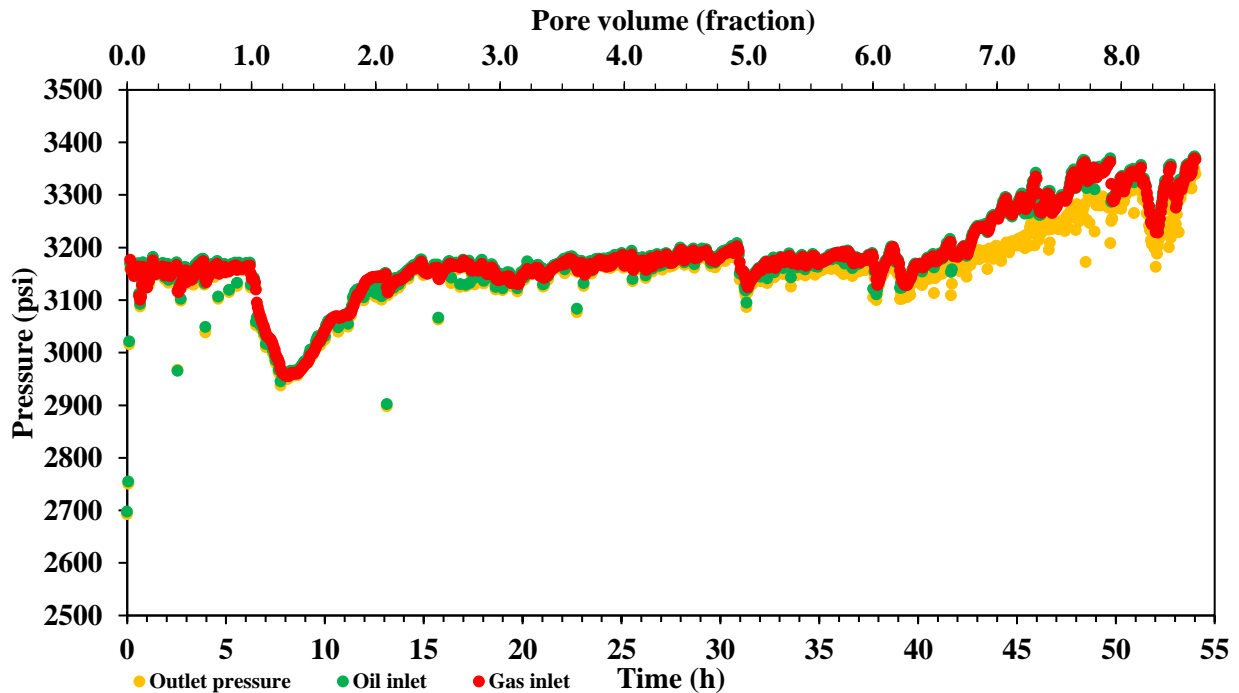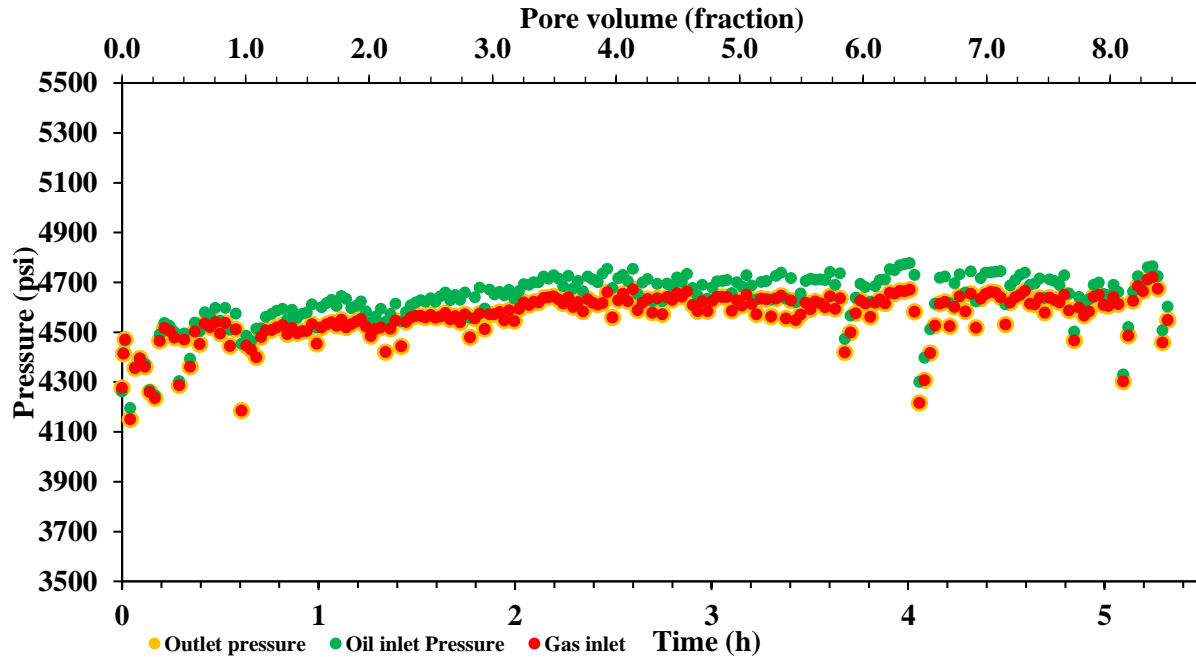
Figure 4.18. Pressures recorded at the oil inlet, gas inlet and outlet of the core sample as function of time and pore volume with a backpressure equal to 4,500 psi (1.07% MMP) at flow rate of 0.25 ml/min.
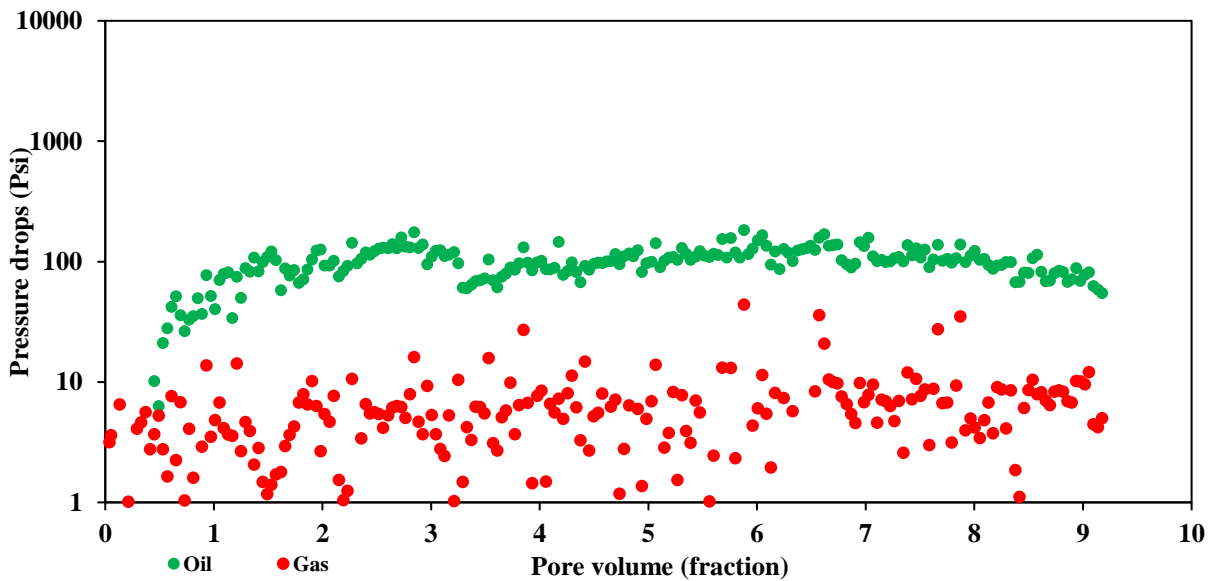
Figure 4.19. Pressure drops recorded for oil and gas across the sample as function of pore volume with a backpressure equal to 3,570 psi (0.85% MMP) at flowrate of 0.25 ml/min.
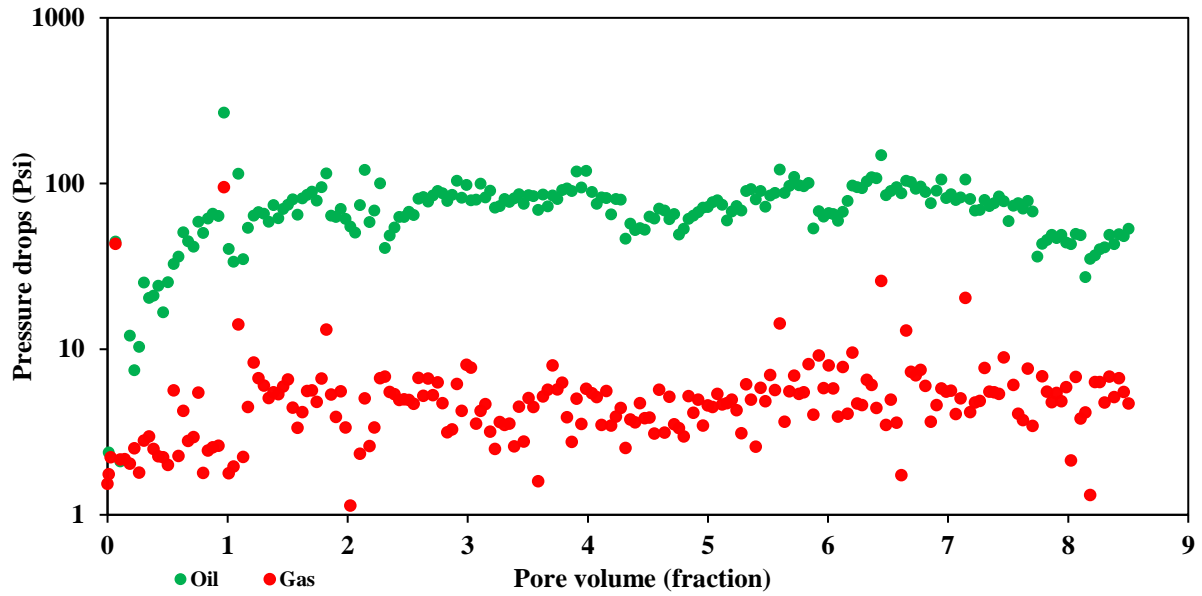
Figure 4.20. Pressure drops recorded of oil and gas across the sample as function of pore volume with a backpressure equal to 4,500 psi (1.07% MMP) at flow rate of 0.25 ml/min.
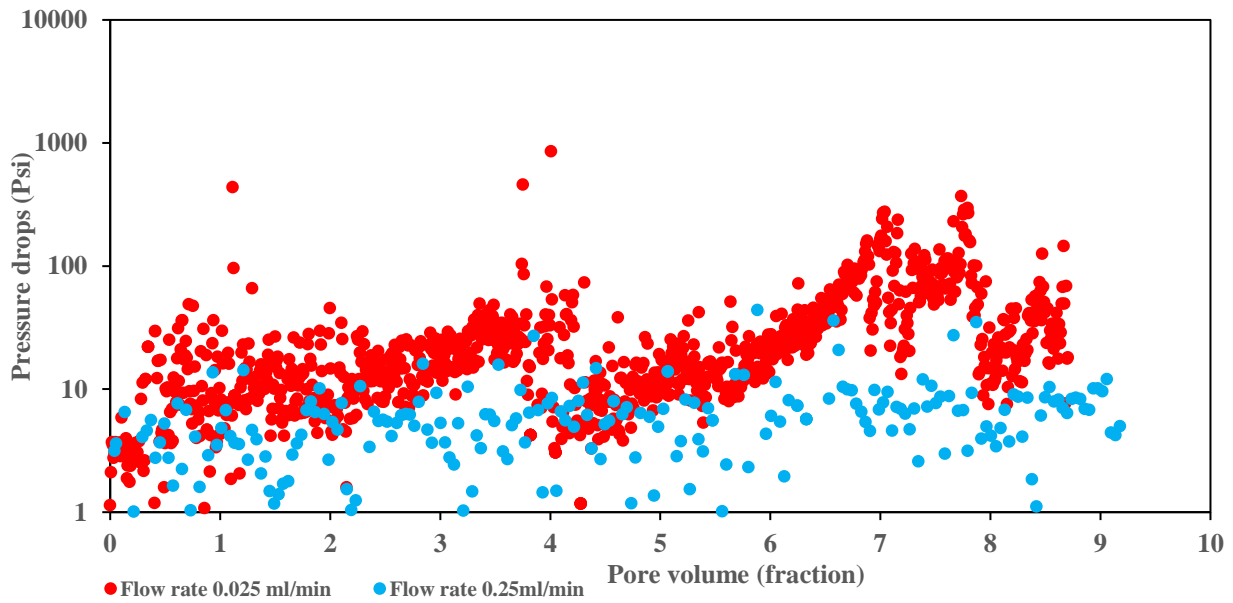
Figure 4.21. Comparison of pressure drops recorded of gas across the sample as function of pore volume with a backpressure equal to 3,570 at flow rates of 0.025 and 0.25 ml/min.
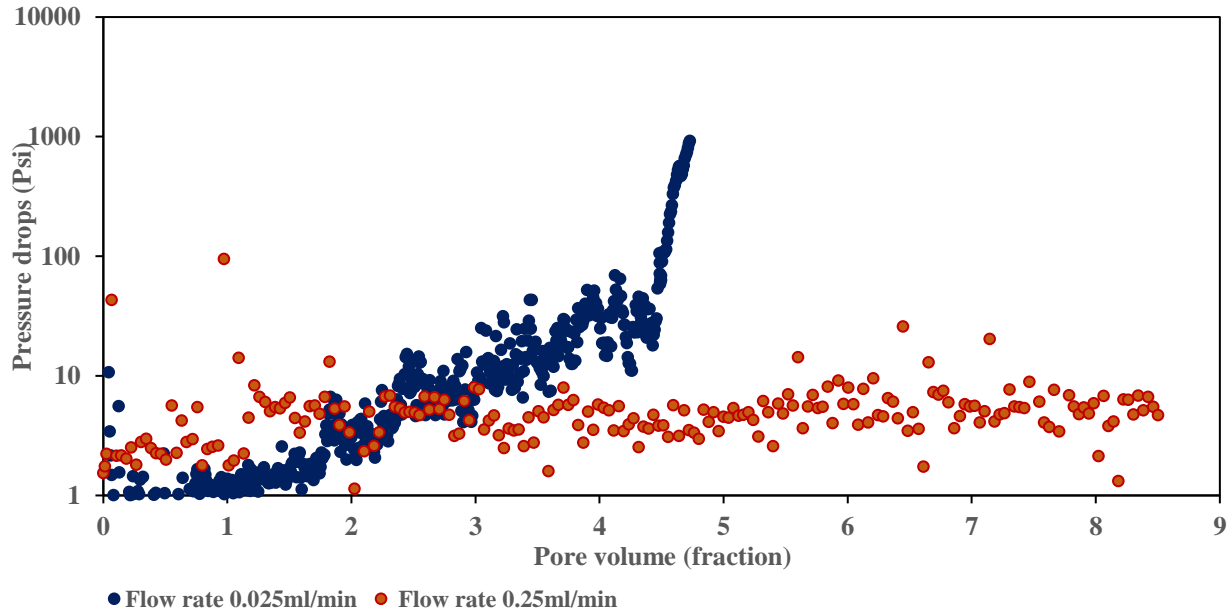
Figure 4.22. Comparison of pressure drops recorded of gas across the sample as function of pore volume with a backpressure equal to 4,500 psi at flow rates of 0.025 and 0.25 ml/min.

The fact that flowing oil and gas at different flowrates lead to to different results indicate that the remaining crude solids content are not playing a major role in the permeability impairment.

4.4. Evaluation of the efficacy of surfactants injection to prevent asphaltene accumulation

4.4.1. Sample preparation

The sample preparation for the experiments is fairly similar to the sample preparation used for the experiments investigating the impact of pressure and flowrate on asphaltenes accumulation. However, in this case, the sample is initially saturated with brine containing 1 gpt and 10 gpt of a nonionic surfactant. The saturated core plug is flooded with 4 to 6 pore volumes of crude oil at constant pressure of 4,500 psi to establish S_{wir} (Figure 4.23). Figure 4.24 shows S_{wir} ranged

between 31.7% and 33.9% before the evaluation of surfactant treatment to prevent formation damage due to asphaltenes accumulation.
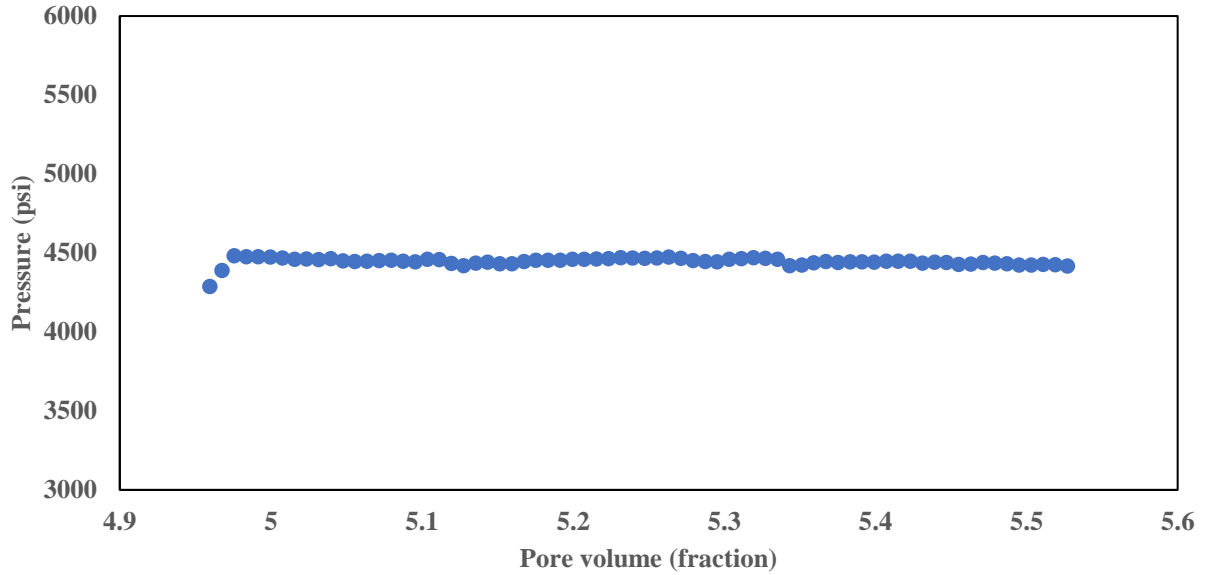
Figure 4.23. Pressures recorded at the oil inlet of the core sample as function of pore volume with a backpressure equal to 4,500 psi (1.07% MMP) and flowrate of 0.025 ml/min.
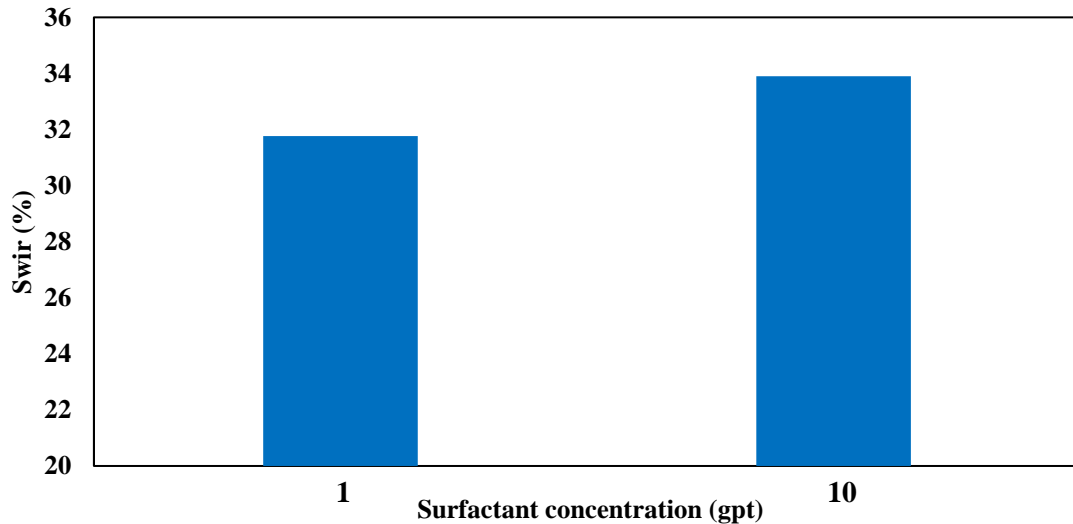
**Figure 4.24. S_{wir} values obtained prior to the evaluation of surfactant injection to prevent formation damage due to asphaltenes accumulation. An average S_{wir} of 32.84 ± 1.07 was obtained for these experiments.**

Figure 4.25 shows the pictures of oil droplet in contact with the core sample after saturation with brine containing 1 GPT of surfactant with a contact angle close to 32° measured.
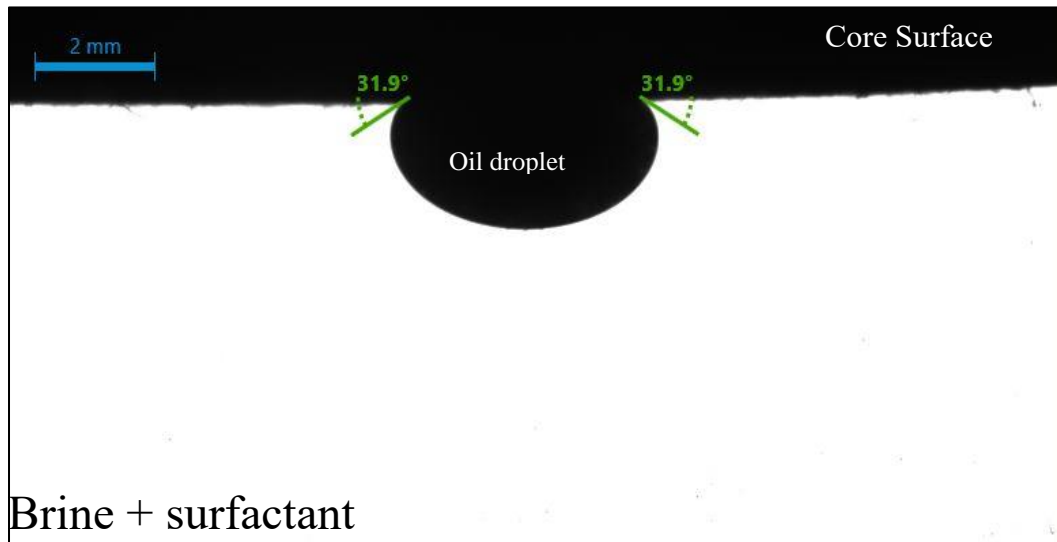
Figure 4.25. Contact angle measurement between an oil droplet and the Berea core plug saturated with 1gpt surfactant solution.

The contact angle conducted after the aging step is illustrated on Figure 4.26. After aging, the contact angle between the oil droplet and the core sample increased to 137°. This contact angle value demonstrates that even when the core is previously saturated with brine containing surfactant, the aging process can successfully alter the wettability of the core sample to oil wet.
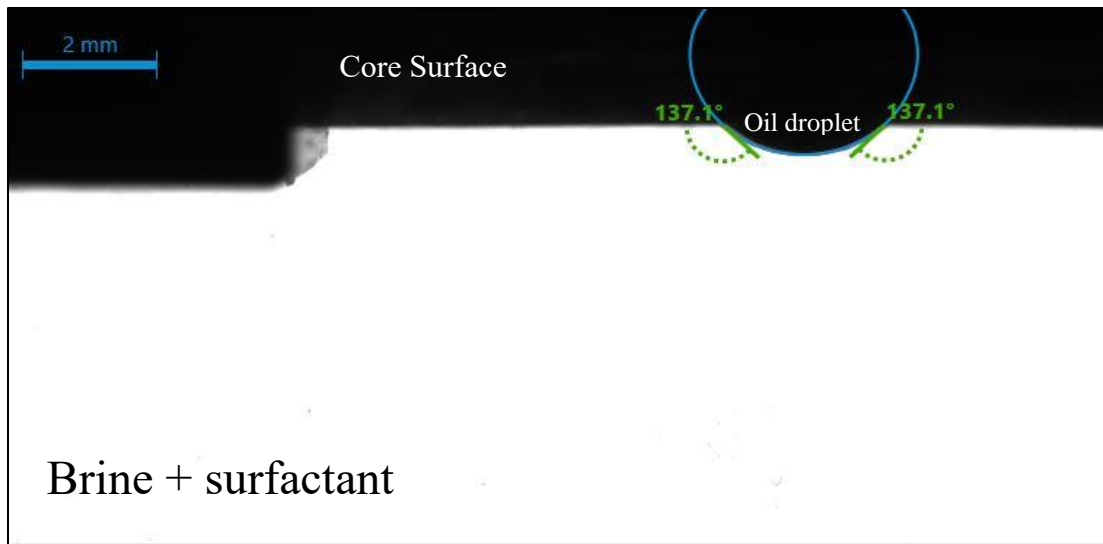
Figure 4.26. Post aging contact angle measurement between an oil droplet and the core plug initially saturated with brine containing 1 GPT of surfactant.

4.4.2. Results of the impact of surfactants on asphaltene accumulation

In these experiments, the core samples were initially saturated with brine and surfactant solutions at 1 and 10 GPT in order to evaluate their ability to mitigate the asphaltenes accumulation. For both experiments, we injected gas and oil at 4,500 psi, at a flowrate of 0.025 ml/min and a constant temperature of 170°F. These pressures and flowrates were the conditions at which we observed the largest permeability impairment due to asphaltenes accumulation. A Reynold number of 0.011 was computed for these experiments.

Figure 4.27 and Figure 4.28 illustrate the recorded oil inlet, gas inlet and outlet pressures for the experiments with 1 gpt and 10 gpt respectively.
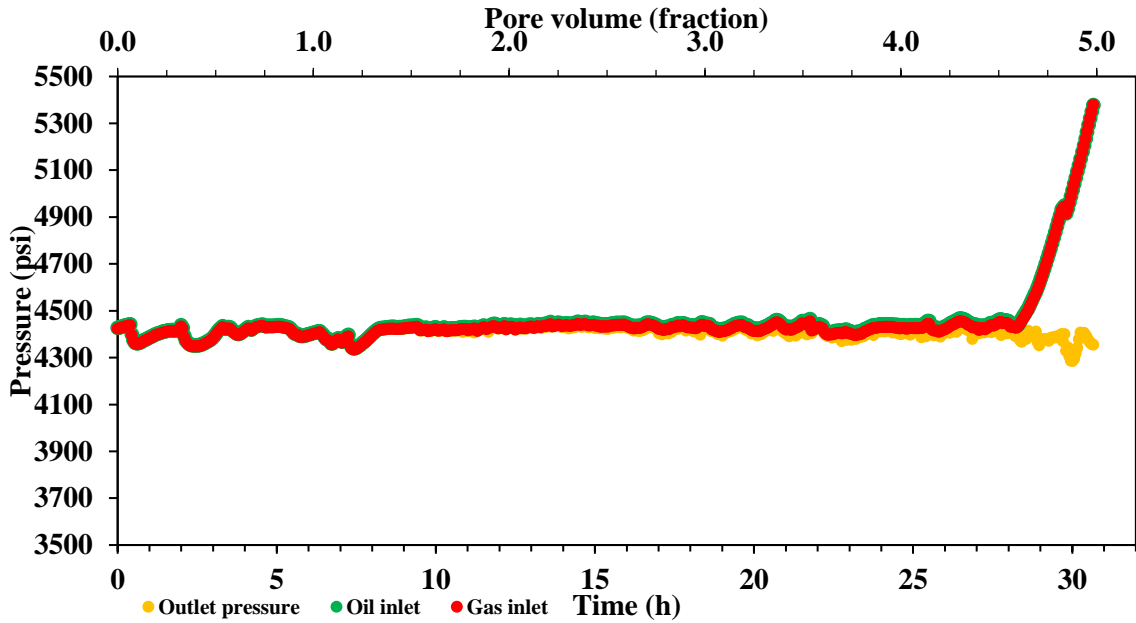
Figure 4.27. Pressures recorded at the oil inlet, gas inlet and outlet of the core sample as function of time and pore volume with a backpressure equal to 4,500 psi (1.07% MMP) at a flowrate of 0.025 ml/min and 1 gpt surfactant.
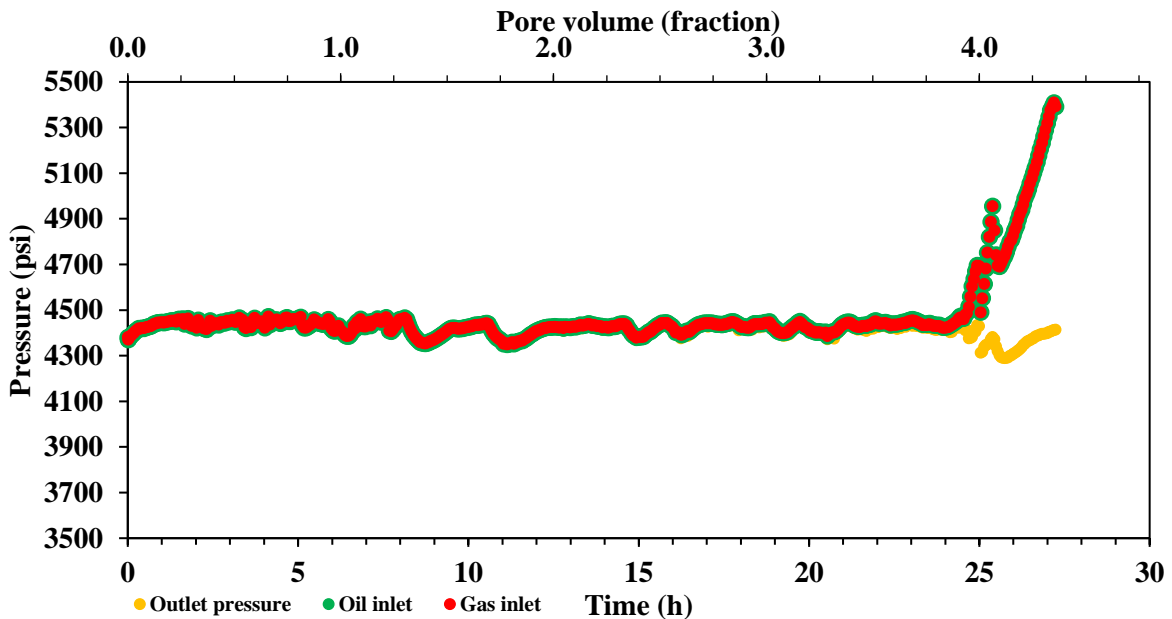

Figure 4.28. Pressures recorded at the oil inlet, gas inlet and outlet of the core sample as function of time and pore volume with a backpressure equal to 4,500 psi (1.07% MMP) at flow rate of 0.025 ml/min and 10 gpt surfactant.

For both experiments, the pressures are initially constant before a sudden increase in the oil and gas inlet pressures that lead to the interruption of the experiments when the pressures reached 5,400 psi. This increase occurred at 4.6 pore volumes for the experiments with 1 gpt and 4 pore volumes for the experiment with 10 gpt. These increases in the inlet pressures while the outlet pressures were constant indicate a permeability impairment due to asphaltene accumulation in the sample (Figure 4.29 and Figure 4.30).
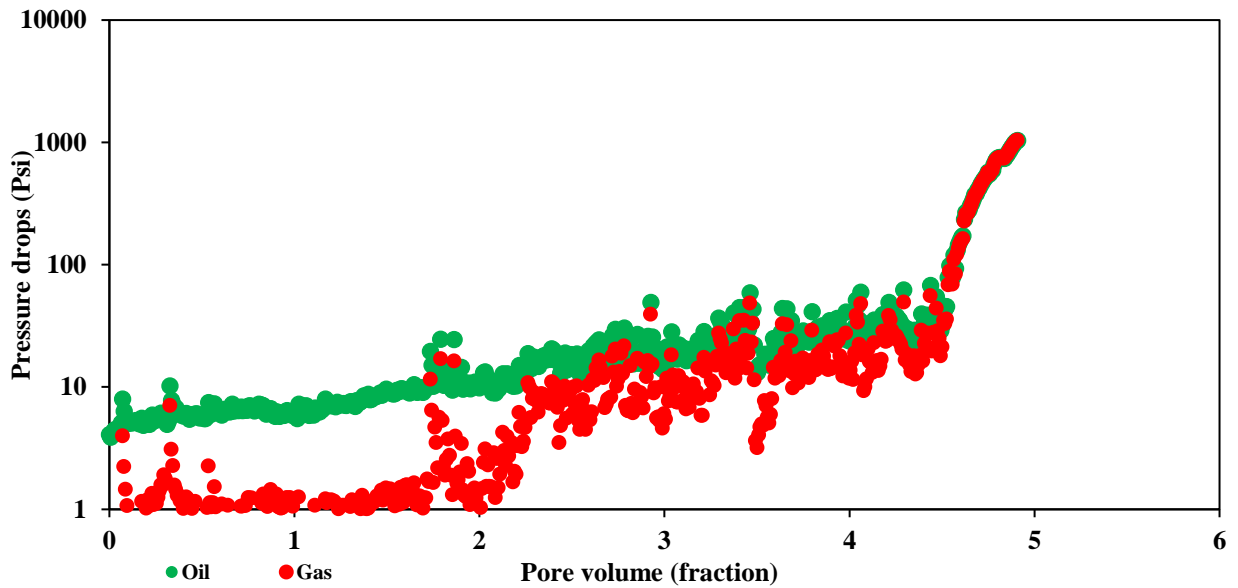
Figure 4.29. Pressure drops recorded of oil and gas across the sample as function of pore volume with a backpressure equal to 4,500 psi (1.07% MMP) at flowrate of 0.025 ml/min and 1 gpt of surfactant.
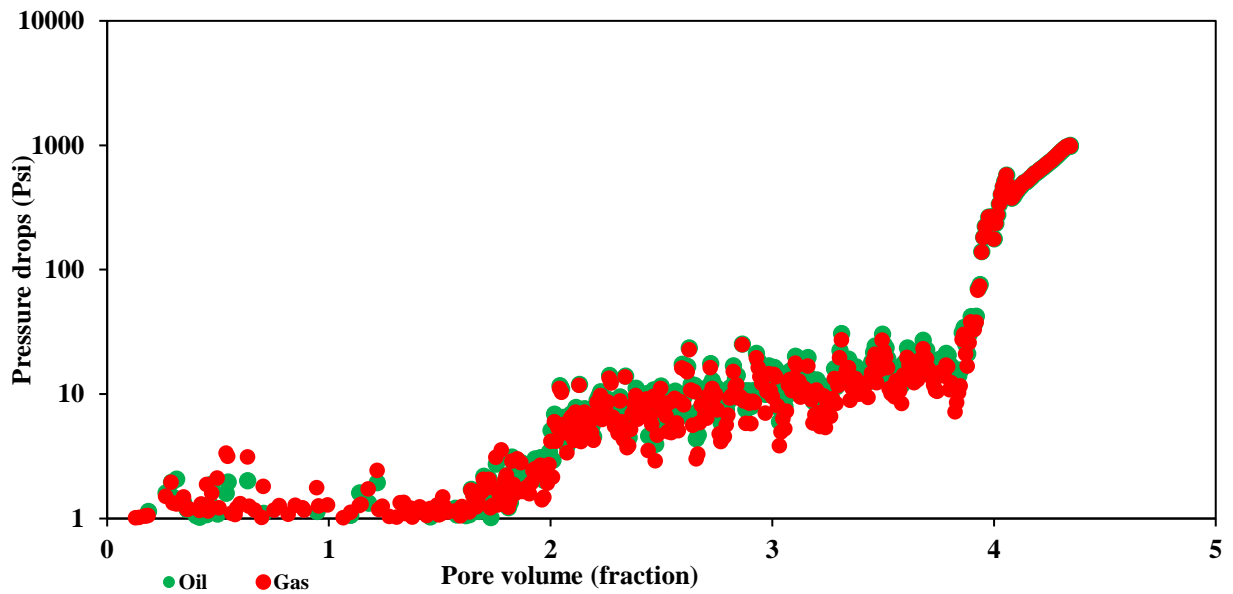
Figure 4.30. Pressure drops recorded of oil and gas across the sample as function of pore volume with a backpressure equal to 4,500 psi (1.07% MMP) at flow rate of 0.025 ml/min and 10 gpt of surfactant.

To compare the results of the experiments with and without surfactant we have plotted the oil pressure drops for the experiments with 1 gpt, 10 gpt and with no surfactant in Figure 4.31. This comparison shows that the formation pressure drops profile of the experiments with 1 gpt is similar to the pressure drops profile of the experiment with no surfactant with an increase in pressure at 4.5 pore volumes. However, the experiment with 10 gpt presents an increase in pressure drops at 4 pore volumes indicating that formation damage occurs earlier in the case with 10 gpt than in the cases with 1 gpt and no surfactant.

These results are counter intuitive as we expected the surfactant to delay or prevent the formation damage. We do not have an explanation for these results, but they could constitute a research subject in the future.

59
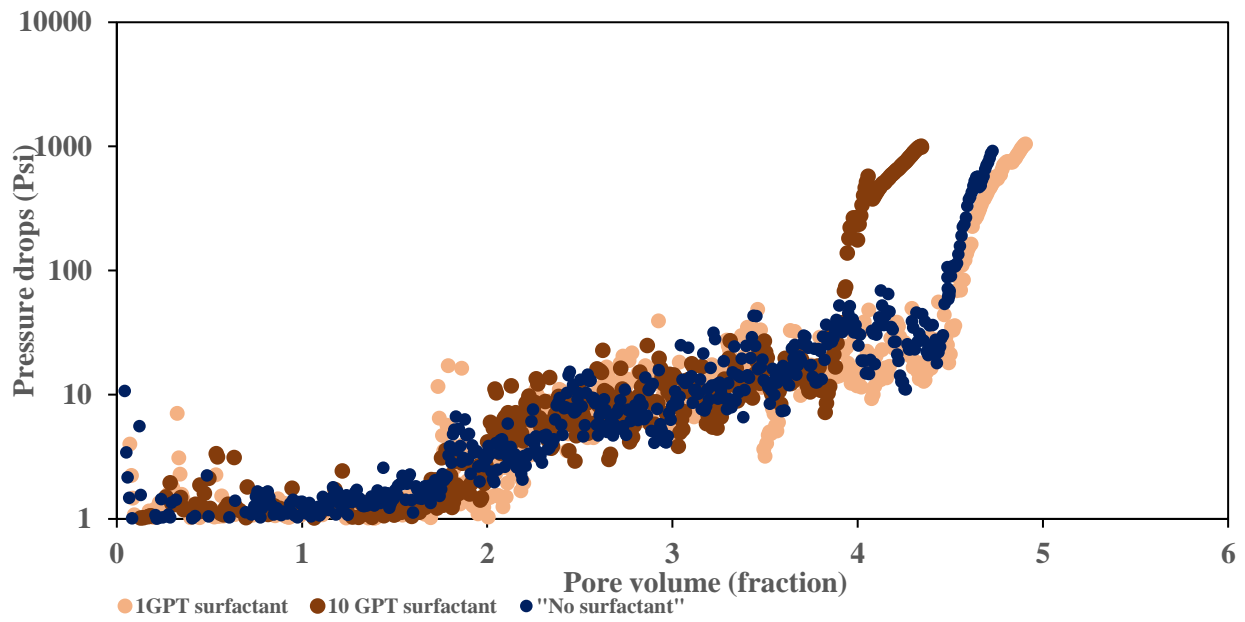
Figure 4.31. Comparison of pressure drops recorded of gas across the sample as function of pore volume with a backpressure equal to 4,500 psi at flow rates of 0.025 ml/min and different surfactant concentrations.

# CHAPTER 5: CONCLUSIONS AND RECOMMENDATIONS

5.1. Conclusion

During this thesis project, we have investigated by means of experimental methods the impacts of reservoir pressures and flowrates on asphaltenes accumulation during oil and gas flow in a Berea sandstone core sample. We have also evaluated the efficacy of surfactant injection to prevent the deposition of asphaltenes. Our investigations revealed that:

- Significant asphaltenes precipitation near the MMP leads to severe formation damage which can be detrimental to production and injection operations. However, asphaltenes accumulation is a slow process that will require at least 4.5 PV to be flown before the occurrence of formation damage.

- Below the MMP, the small amounts of asphaltenes precipitated can reduce reservoir permeability. However, this permeability reduction could be temporary because of the redissolution of the asphaltenes molecules into the crude oil.

- As we increased the flowrate from 0.025ml/min (Reynold number 0.011) to 0.25 ml/min (Reynold number 0.11) asphaltenes accumulation could not be observed regardless of the pressure. Therefore, production or injection flowrate management can be used to prevent formation damage to asphaltenes accumulation.

- The injection of surfactant did not prevent asphaltenes accumulation. Our results show that formation damage occurs faster when the surfactant concentration is increased from 1 gpt to 10 gpt.

5.2. Recommendations

For future studies and a better understanding of asphaltenes accumulation in reservoir rocks, we recommend the following:

- The co-injection of crude oil with more asphaltenes content and the same gas mixture at pressures similar to the pressures used in this study in order to assess the impact of crude oil asphaltene content on the accumulation process.

- More experiments at multiple flowrates between 0.025 ml/min and 0.25 ml/min in order to determine the critical flowrate beyond which formation damage due to asphaltenes accumulation does not occur.

- The development of a sub research program that will investigate the reasons why the injection of surfactant did not prevent asphaltenes accumulation in the core sample.

- Modeling of the experimental data acquired during this thesis in order to understand the underlying mechanisms responsible for asphaltenes accumulation.

- Use adequate mesh size filter vis a vis the core sample pore sizes distribution to reduce the crude oil solid content and avoid possible small pore sizes plugging.

- Quantify the asphaltene content in the core sample after each experiment.

- Design several experiments where the water phase will also flow.

- Conduct core flooding with solutions of 1 gpt and 10 gpt surfactant as a control prior to oil and gas coinjection experiments.

References

Ahmadi, Y., Kharrat, R., Hashemi, A., Bahrami, P., & Mahdavi, S. (2014). The effect of temperature and pressure on the reversibility of asphaltene precipitation. Petroleum science and technology, 32(18), 2263-2273.

Akbarzadeh, K., Hammami, A., Kharrat, A., Zhang, D., Allenson, S., Creek, J., ... & Solbakken, T. (2007). Asphaltenes—problematic but rich in potential. Oilfield Review, 19(2), 22-43.

Ali, L. H., & Al-Ghannam, K. A. (1981). Investigations into asphaltenes in heavy crude oils. I. Effect of temperature on precipitation by alkane solvents. Fuel, 60(11), 1043-1046.

Ali, M. A., & Islam, M. R. (1998). The effect of asphaltene precipitation on carbonate-rock permeability: an experimental and numerical approach. SPE production & facilities, 13(03), 178-183.

Alrashidi, H., Farid Ibrahim, A., & Nasr-El-Din, H. (2018). Bio-Oil Dispersants Effectiveness on AsphalteneSludge During Carbonate Acidizing Treatment. In SPE Trinidad and Tobago Section Energy Resources Conference. OnePetro.

Al-Sahhaf, T. A., Fahim, M. A., & Elkilani, A. S. (2002). Retardation of asphaltene precipitation by addition of toluene, resins, deasphalted oil and surfactants. Fluid phase equilibria, 194, 1045-1057.

Alves, C. A., Romero Yanes, J. F., Feitosa, F. X., & de Sant'Ana, H. B. (2019). Effect of Temperature on Asphaltenes Precipitation: Direct and Indirect Analyses and Phase Equilibrium Study. Energy & Fuels, 33(8), 6921-6928.

Andrews, A. B., Guerra, R. E., Mullins, O. C., & Sen, P. N. (2006). Diffusivity of asphaltene molecules by fluorescence correlation spectroscopy. The Journal of Physical Chemistry A, 110(26), 8093-8097.

Angle, C. W., Long, Y., Hamza, H., & Lue, L. (2006). Precipitation of asphaltenes from solvent-diluted heavy oil and thermodynamic properties of solvent-diluted heavy oil solutions. Fuel, 85(4), 492-506.

Ashoori, S., Sharifi, M., Masoumi, M., & Salehi, M. M. (2017). The relationship between SARA fractions and crude oil stability. Egyptian Journal of Petroleum, 26(1), 209-213.

Ballard, B. D. (2007, November). Quantitative mineralogy of reservoir rocks using Fourier transform infrared spectroscopy. In SPE Annual Technical Conference and Exhibition. OnePetro.

Bearsley, S., Forbes, A., & G. HAVERKAMP, R. (2004). Direct observation of the asphaltene structure in paving-grade bitumen using confocal laser-scanning microscopy. Journal of microscopy, 215(2), 149-155.

Behbahani, T. J., Ghotbi, C., Taghikhani, V., & Shahrabadi, A. (2014). Investigation of asphaltene adsorption in sandstone core sample during CO2 injection: Experimental and modified modeling. Fuel, 133, 63-72.

Behbahani, T. J., Ghotbi, C., Taghikhani, V., & Shahrabadi, A. (2015). Experimental study and mathematical modeling of asphaltene deposition mechanism in core samples. Oil & Gas Science and Technology–Revue d'IFP Energies nouvelles, 70(6), 1051-1074.

Boek, E. S., Wilson, A. D., Padding, J. T., Headen, T. F., & Crawshaw, J. P. (2010). Multi-scale simulation and experimental studies of asphaltene aggregation and deposition in capillary flow. Energy & Fuels, 24(4), 2361-2368.

Boussingault JB: "Memoire sur la composition des bitumens," Annales de Chimie et de Physique64 (1837).

Buckley, J. S. (1996). Microscopic investigation of the onset of asphaltene precipitation. Fuel science and technology international, 14(1-2), 55-74.

Buckley, J. S., & Wang, J. (2002). Crude oil and asphaltene characterization for prediction of wetting alteration. Journal of Petroleum Science and Engineering, 33(1-3), 195-202.

Burke, N. E., Hobbs, R. D., & Kashou, S. F. (1988). Measurement and modeling of asphaltene precipitation from live reservoir fluid systems. In Annual technical conference and exhibition (pp. 113-126).

Chandio, Z. A., Ramasamy, M., & Mukhtar, H. B. (2015). Temperature effects on solubility of asphaltenes in crude oils. Chemical Engineering Research and Design, 94, 573-583.

Chen, W., Guo, T., Kapoor, Y., Russell, C., Juyal, P., Yen, A., & Hartman, R. L. (2019). An automated microfluidic system for the investigation of asphaltene deposition and dissolution in porous media. Lab on a Chip, 19(21), 3628-3640.

Cimino, R., Correra, S., Del Bianco, A., & Lockhart, T. P. (1995). Solubility and phase behavior of asphaltenes in hydrocarbon media. In asphaltenes (pp. 97-130). Springer, Boston, MA.

Clementz, D. M. (1982). Alteration of rock properties by adsorption of petroleum heavy ends: implications for enhanced oil recovery. In SPE Enhanced Oil Recovery Symposium. One Petro.

Dasari, S. R., & Goud, V. V. (2014). Effect of pre-treatment on solvents extraction and physicochemical properties of castor seed oil. Journal of Renewable and Sustainable Energy, 6(6), 063108.

Fakher, S., & Imqam, A. (2019). Asphaltene precipitation and deposition during CO2 injection in nano shale pore structure and its impact on oil recovery. Fuel, 237, 1029-1039.

Fakher, S., Ahdaya, M., Elturki, M., & Imqam, A. (2020). Critical review of asphaltene properties and factors impacting its stability in crude oil. *Journal of Petroleum Exploration and Production Technology*, *10*(3), 1183-1200.

Gonzalez, D. L., Hirasaki, G. J., Creek, J., & Chapman, W. G. (2007). Modeling of asphaltene precipitation due to changes in composition using the perturbed chain statistical associating fluid theory equation of state. Energy & fuels, 21(3), 1231-1242.

Goual, L. (2012). Petroleum asphaltenes. Crude oil emulsions—composition stability and characterization, ed. ME Abdul-Raouf, 27-42.

Gray, M. R., Tykwinski, R. R., Stryker, J. M., & Tan, X. (2011). Supramolecular assembly model for aggregation of petroleum asphaltenes. Energy & Fuels, 25(7), 3125-3134.

Hashemi, R., Kshirsagar, L. K., Nandi, S., Jadhav, P. B., & Golab, E. G. (2019). EXPERIMENTAL AND CMG STUDY OF ASPHALTENE PRECIPITATION UNDER NATURAL DEPLETION AND GAS INJECTION CONDITIONS. Petroleum & Coal, 61(2).

Hashmi, S. M., & Firoozabadi, A. (2013). Self-assembly of resins and asphaltenes facilitates asphaltene dissolution by an organic acid. Journal of colloid and interface science, 394, 115-123.

Hashmi, S. M., Loewenberg, M., & Firoozabadi, A. (2015). Colloidal asphaltene deposition in laminar pipe flow: Flow rate and parametric effects. Physics of Fluids, 27(8), 083302.

Hashmi, S. M., Zhong, K. X., & Firoozabadi, A. (2012). Acid–base chemistry enables reversible colloid-to-solution transition of asphaltenes in non-polar systems. Soft Matter, 8(33), 8778-8785.

Haynes, C. D., & Gray, K. E. (1974). Sand particle transport in perforated casing. Journal of Petroleum Technology, 26(01), 80-84.

Headen, T. F., Boek, E. S., & Skipper, N. T. (2009). Evidence for asphaltene nanoaggregation in toluene and heptane from molecular dynamics simulations. Energy & Fuels, 23(3), 1220-1229.

Hirschberg, A., deJong, L. N., Schipper, B. A., & Meijer, J. G. (1984). Influence of temperature and pressure on asphaltene flocculation. Society of Petroleum Engineers Journal, 24(03), 283-293.

Hirschberg, A., deJong, L. N., Schipper, B. A., & Meijer, J. G. (1984). Influence of temperature and pressure on asphaltene flocculation. Society of Petroleum Engineers Journal, 24(03), 283-293.

Jafari Behbahani, T., Ghotbi, C., Taghikhani, V., & Shahrabadi, A. (2012). Investigation on asphaltene deposition mechanisms during CO2 flooding processes in porous media: a novel experimental study and a modified model based on multilayer theory for asphaltene adsorption. Energy & fuels, 26(8), 5080-5091.

Jafari Behbahani, T., Ghotbi, C., Taghikhani, V., & Shahrabadi, A. (2012). Investigation on asphaltene deposition mechanisms during CO2 flooding processes in porous media: a novel experimental study and a modified model based on multilayer theory for asphaltene adsorption. Energy & Fuels, 26(8), 5080-5091.

Khorgami, Z., Shoar, S., Anbara, T., Soroush, A., Nasiri, S., Movafegh, A., & Aminian, A. (2014). A randomized clinical trial comparing 4-port, 3-port, and single-incision laparoscopic cholecystectomy. Journal of investigative surgery, 27(3), 147-154.

Kord, S., Miri, R., Ayatollahi, S., & Escrochi, M. (2012). Asphaltene deposition in carbonate rocks: experimental investigation and numerical simulation. Energy & fuels, 26(10), 6186-6199.

Kord, S., Mohammadzadeh, O., Miri, R., & Soulgani, B. S. (2014). Further investigation into the mechanisms of asphaltene deposition and permeability impairment in porous media using a modified analytical model. Fuel, 117, 259-268.

Kordestany, A., Hassanzadeh, H., & Abedi, J. (2019). An experimental approach to investigating permeability reduction caused by solvent-induced asphaltene deposition in porous media. The Canadian Journal of Chemical Engineering, 97(1), 361-371.

Leontaritis, K. J. (1996). The asphaltene and wax deposition envelopes. Fuel Science and Technology International, 14(1-2), 13-39.

Leontaritis, K. J., & Mansoori, G. A. (1987). Asphaltene flocculation during oil production and processing: A thermodynamic collodial model. In SPE International Symposium on Oilfield Chemistry. OnePetro.

Leontaritis, K. J., Amaefule, J. O., & Charles, R. E. (1994). A systematic approach for the prevention and treatment of formation damage caused by asphaltene deposition. SPE Production & facilities, 9(03), 157-164.

Lin, Y. J., He, P., Tavakkoli, M., Mathew, N. T., Fatt, Y. Y., Chai, J. C., ... & Biswal, S. L. (2017). Characterizing asphaltene deposition in the presence of chemical dispersants in porous media micromodels. Energy & Fuels, 31(11), 11660-11668.

Lin, Y. J., He, P., Tavakkoli, M., Mathew, N. T., Fatt, Y. Y., Chai, J. C., ... & Biswal, S. L. (2017). Characterizing asphaltene deposition in the presence of chemical dispersants in porous media micromodels. Energy & Fuels, 31(11), 11660-11668.

Maqbool, T., Srikiratiwong, P., & Fogler, H. S. (2011). Effect of temperature on the precipitation kinetics of asphaltenes. Energy & fuels, 25(2), 694-700.

Mendoza de la Cruz, J. L., Arguelles-Vivas, F. J., Matias-Perez, V., Durán-Valencia, C. D. L. A., & Lopez-Ramirez, S. (2009). Asphaltene-induced precipitation and deposition during pressure depletion on a porous medium: an experimental investigation and modeling approach. Energy & Fuels, 23(11), 5611-5625.

Mendoza de la Cruz, J. L., Arguelles-Vivas, F. J., Matias-Perez, V., Durán-Valencia, C. D. L. A., & Lopez-Ramirez, S. (2009). Asphaltene-induced precipitation and deposition during pressure depletion on a porous medium: an experimental investigation and modeling approach. Energy & Fuels, 23(11), 5611-5625.

Minssieux, L. (1997). Core damage from crude asphaltene deposition. In International Symposium on Oilfield Chemistry. OnePetro.

Mirzayi, B., Vafaie-Sefti, M., Mousavi-Dehghani, S. A., Fasih, M., & Mansoori, G. A. (2008). The effects of asphaltene deposition on unconsolidated porous media properties during miscible natural gas flooding. Petroleum science and technology, 26(2), 231-243.

Moradi, S., Rashtchian, D., GANJEH, G. M., Emadi, M. A., & Dabir, B. (2012). Experimental investigation and modeling of asphaltene precipitation due to gas injection.

Mullins, O. C. (2011). The asphaltenes. Annual Review of Analytical Chemistry, 4, 393-418.

Mullins, O. C., Sabbah, H., Eyssautier, J., Pomerantz, A. E., Barré, L., Andrews, A. B., ... & Zare, R. N. (2012). Advances in asphaltene science and the Yen–Mullins model. Energy & Fuels, 26(7), 3986-4003.

Pak, T., Kharrat, R., Bagheri, M., Khalili, M., & Hematfar, V. (2011). Experimental study of asphaltene deposition during different production mechanisms. Petroleum science and technology, 29(17), 1853-1863.

Riazi, M., & Zare, K. (2018). Influences of Asphaltene Deposition on Formation Damage and Gas Coning. Biomedical Journal of Scientific & Technical Research, 3(5), 3561-3565.

Sanada, A., & Miyagawa, Y. (2006). A case study of a successful chemical treatment to mitigate asphaltene precipitation and deposition in light crude oil field. In SPE Asia Pacific Oil & Gas Conference and Exhibition. OnePetro.

Sondergeld, C. H., & Rai, C. S. (1993). A new concept in quantitative core characterization. The Leading Edge, 12(7), 774-779.

Speight, J. G. (1996). Asphaltenes in crude oil and bitumen: structure and dispersion.

Speight, J. G., & Plancher, H. (1991). Molecular models for petroleum asphaltenes and implications for asphalt science and technology. In Proceedings of the International Symposium on the Chemistry of Bitumens (p. 154).

Struchkov, I. A., Rogachev, M. K., Kalinin, E. S., & Roschin, P. V. (2019). Laboratory investigation of asphaltene-induced formation damage. Journal of Petroleum Exploration and Production Technology, 9(2), 1443-1455.

Thawer, R., Nicoll, D. C., & Dick, G. (1990). Asphaltene deposition in production facilities. Spe production engineering, 5(04), 475-480.

Thomas, F. B., Bennion, D. B., Bennion, D. W., & Hunter, B. E. (1992). Experimental and theoretical studies of solids precipitation from reservoir fluid. Journal of Canadian Petroleum Technology, 31(01).

Waller, P. R., Williams, A., & Bartle, K. D. (1989). The structural nature and solubility of residual fuel oil fractions. Fuel, 68(4), 520-526.

Wang, J. (2000). Asphaltene: A general introduction. New Mexico.

Wang, J., Buckley, J. S., & Creek, J. L. (2004). Asphaltene deposition on metallic surfaces. Journal of dispersion science and technology, 25(3), 287-298.

Wang, S., & Civan, F. (2000). Field simulation of asphaltene deposition for asphaltenic petroleum reservoirs.

Wang, S., & Civan, F. (2001). Productivity decline of vertical and horizontal wells by asphaltene deposition in petroleum reservoirs. In SPE International Symposium on Oilfield Chemistry. Society of Petroleum Engineers.

Yarranton, H. W. (2005). Asphaltene self-association. Journal of dispersion science and technology, 26(1), 5-8.

Yarranton, H. W., Ortiz, D. P., Barrera, D. M., Baydak, E. N., Barré, L., Frot, D., ... & Oake, J. (2013). On the size distribution of self-associated asphaltenes. Energy & fuels, 27(9), 5083-5106.

Zekri, A. Y., & Almehaideb, R. A. (2001). A novel technique to treat asphaltene deposition in carbonate rocks. In SPE Asia Pacific Oil and Gas Conference and Exhibition. OnePetro.